Bondi-Hoyle-Littleton

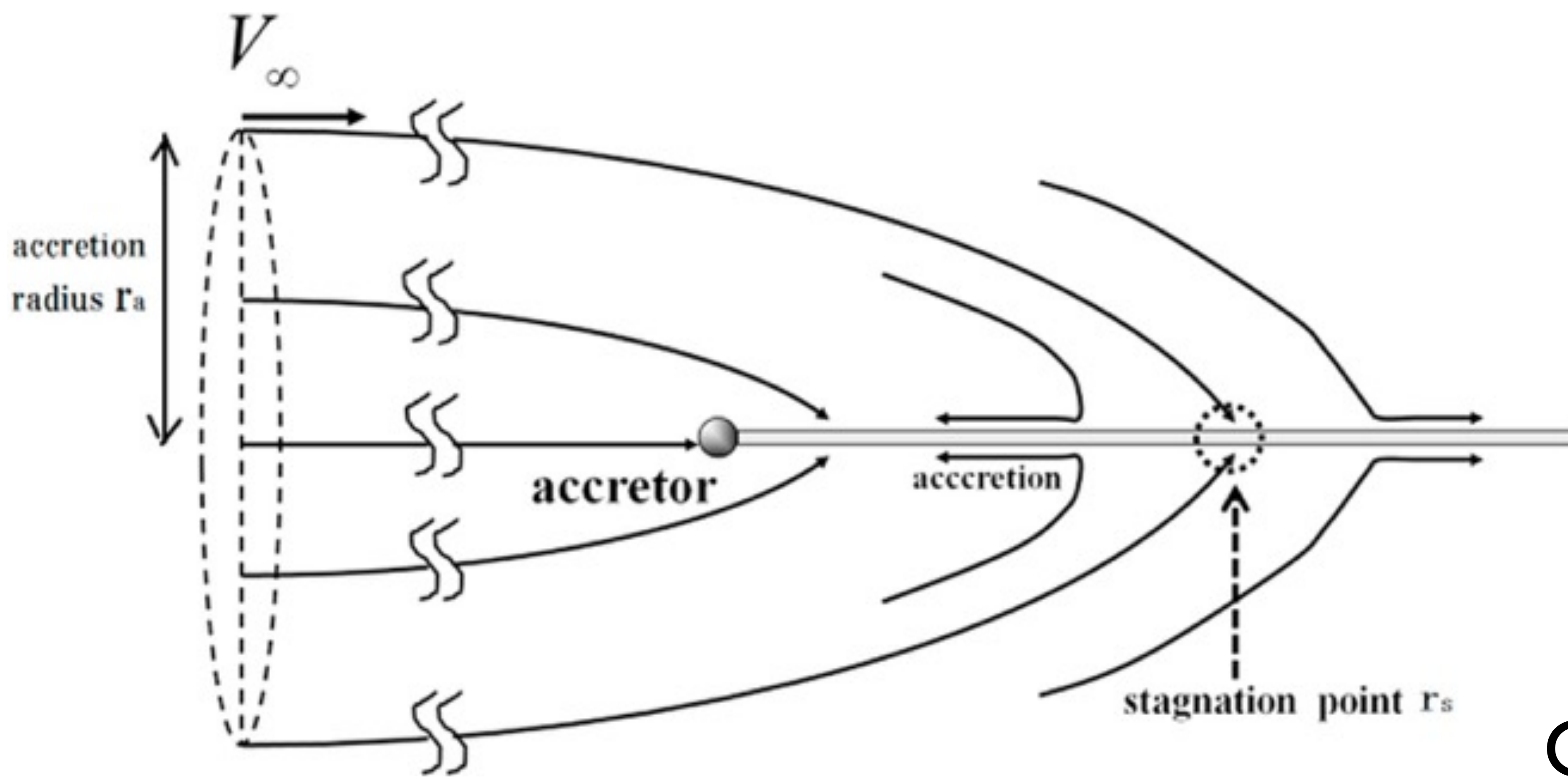

Ohsugi 2018

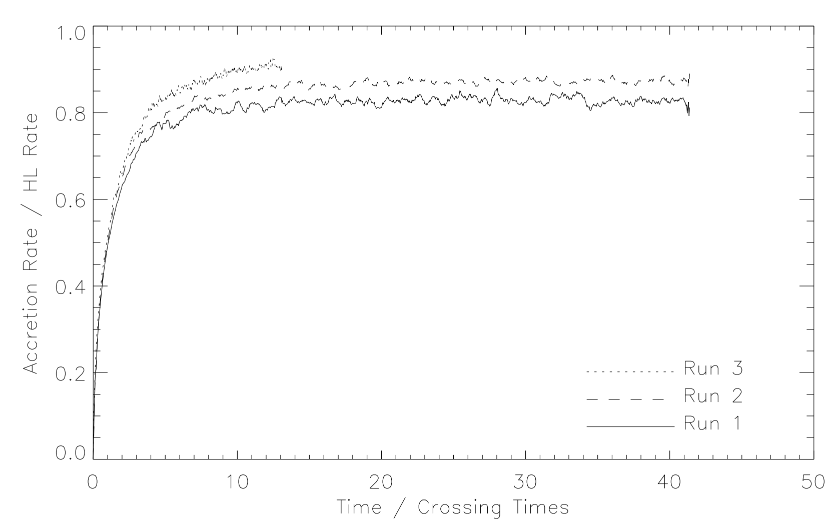

Edgar 2004

Fig. 7. Accretion rates for plain Bondi–Hoyle–Lyttleton flow. The crossing time corresponds to ζ_{HL}

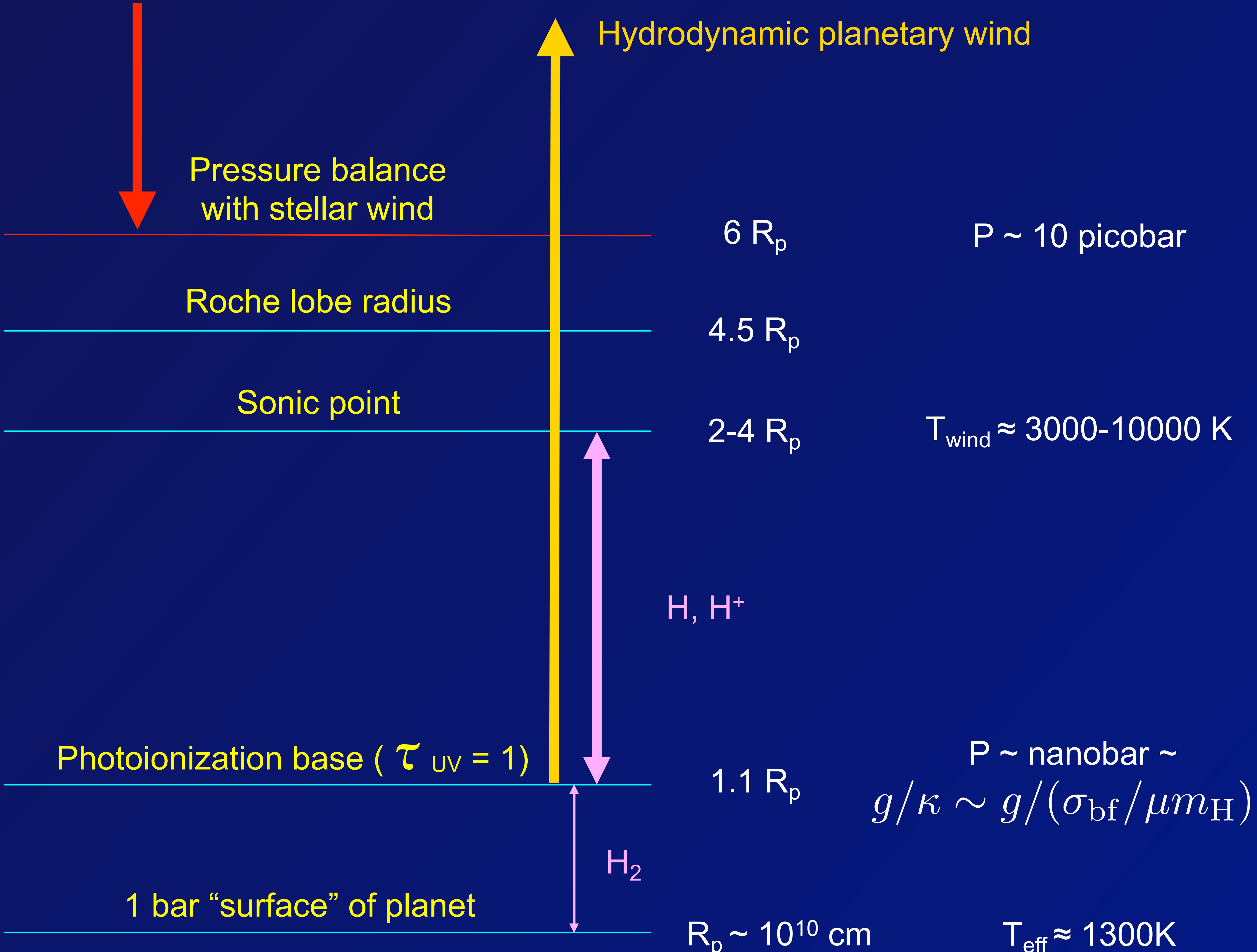

Murray-Clay, EC, & Murray 09

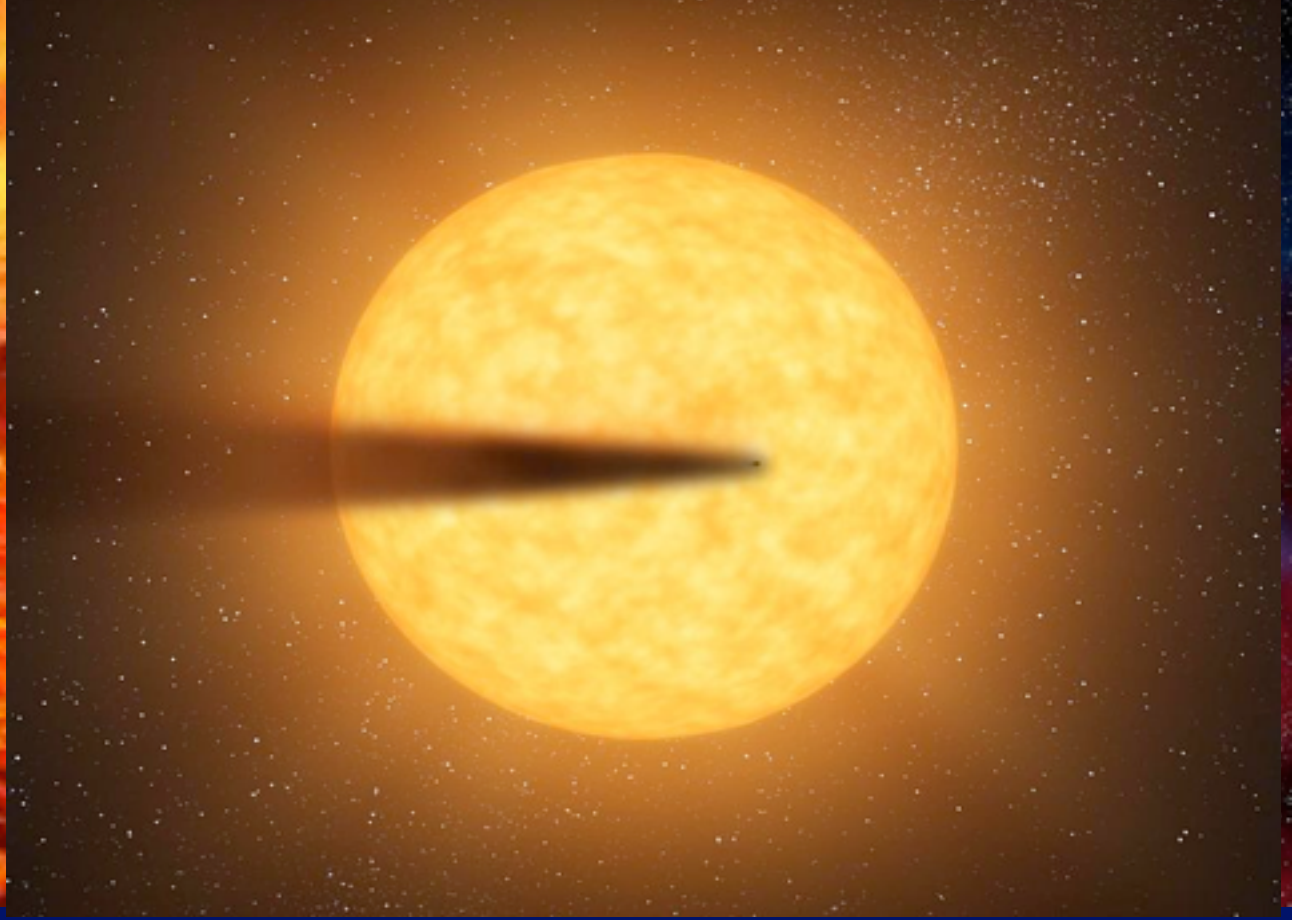

A disintegrating Super-Moon

- Opacity must be due to grains
- Coriolis force + stellar radiation pressure creates trailing tail
- Tail causes prolonged egress
- Scattered light off head of "comet" causes pre-ingress bump

Rappaport, Levine, EC+ 12

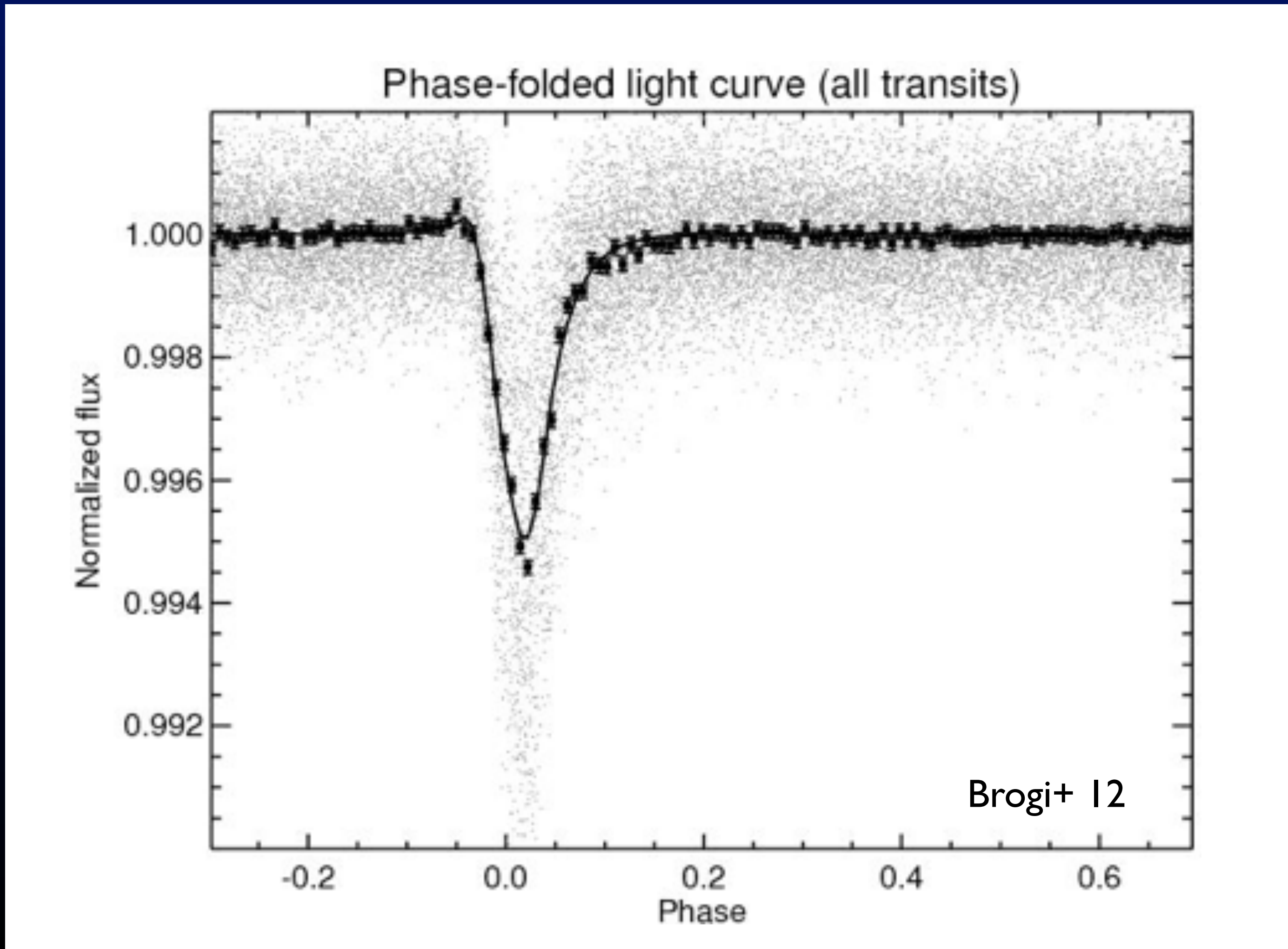

Hydrodynamic model (Perez-Becker + EC 13)

(1D) Mass, momentum, and energy conservation

$$\frac{\partial}{\partial r}(r^2 \rho v) = 0$$

$$\rho v \frac{\partial v}{\partial r} = -\frac{\partial P}{\partial r} - \frac{G M_{\rm p} \rho}{r^2} + \frac{3 G M_\star \rho r}{a^3}$$

- $-\frac{\partial P}{\partial r}$: pressure gradient force
- $-\frac{G M_{\rm p} \rho}{r^2}$: gravitational attraction from planet
- $+\frac{3 G M_\star \rho r}{a^3}$: centrifugal force & attraction from star

$$\rho v \frac{\partial}{\partial r}\left[\frac{kT}{(\gamma - 1)\mu}\right] = \frac{kTv}{\mu}\frac{\partial \rho}{\partial r} + \Gamma$$

- $\rho v \frac{\partial}{\partial r}\left[\frac{kT}{(\gamma - 1)\mu}\right]$: change in internal thermal energy
- $\frac{kTv}{\mu}\frac{\partial \rho}{\partial r}$: PdV work cooling
- $+\Gamma$: heating from dust-gas collisions & latent heat from condensing grains

Mass-loss history

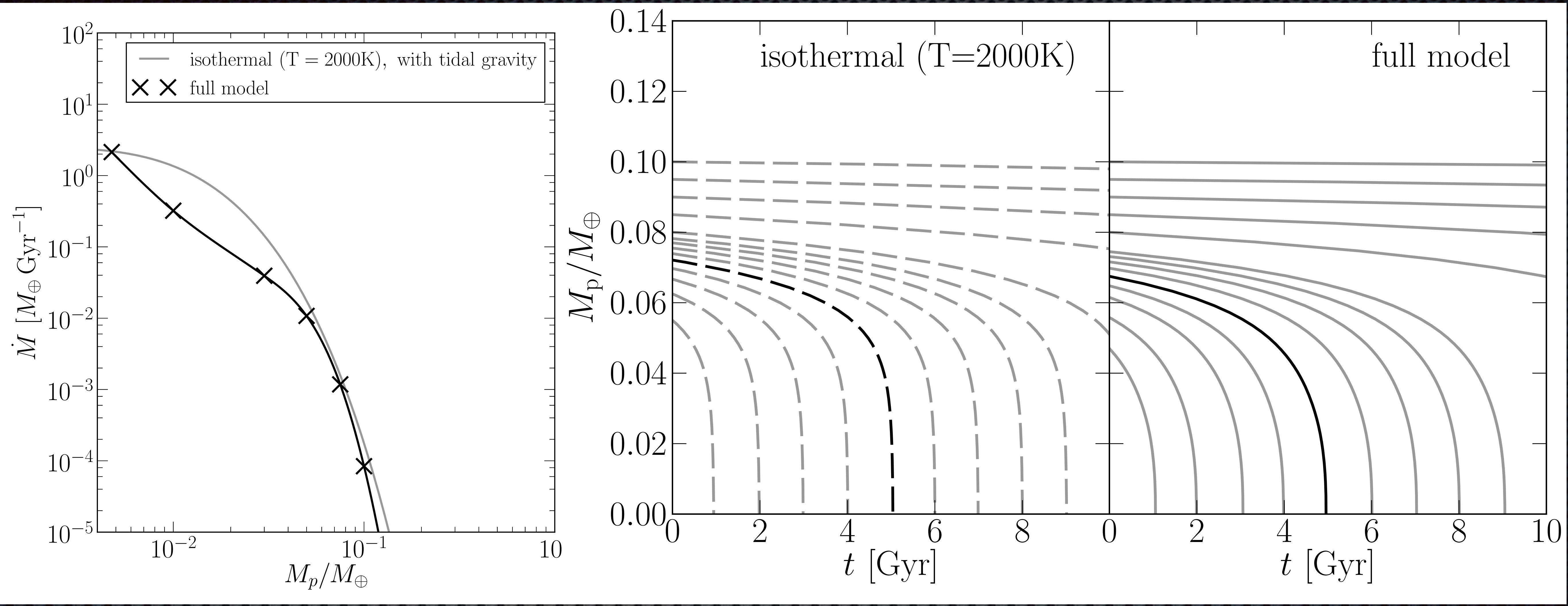

- Little orbital evolution from mass loss; in-situ formation possible
- Catastrophic phase 1/1000 of lifetime
- Observed in 1/150,000 stars: ~1/25 of stars could have a close-in super-Mercury

Perez-Becker + EC 2013

Photoevaporation of planet atmospheres and the creation of the "Fulton gap"

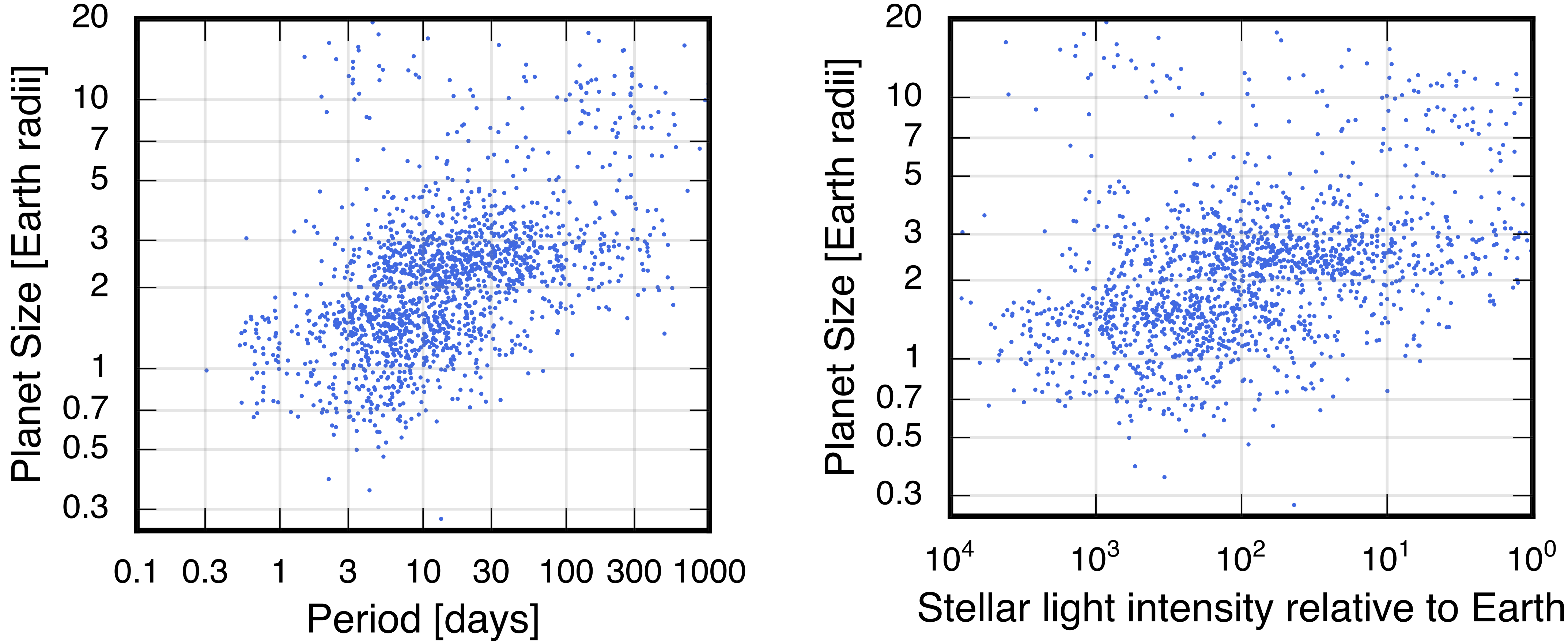

Figure 4. *Left:* distribution of planet radii and orbital periods. *Right:* same as *left* but with insolation flux relative to Earth on the horizontal axis. In both plots, an underdensity of points appears between 1.5 and 2.0 $R_\oplus$.

Galactic magnetic field (M51)

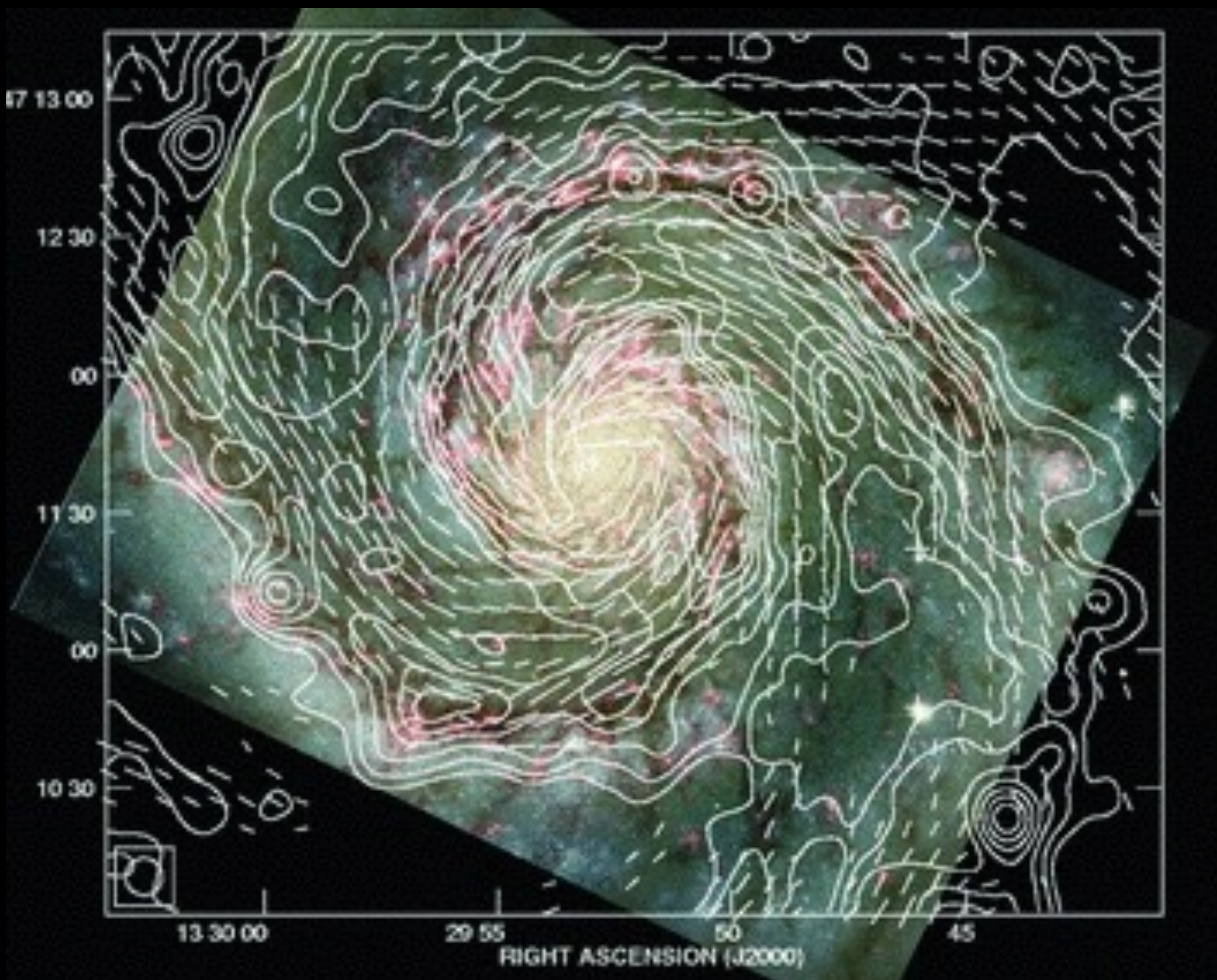

B-direction from linearly polarized radio emission

B-magnitude in microG

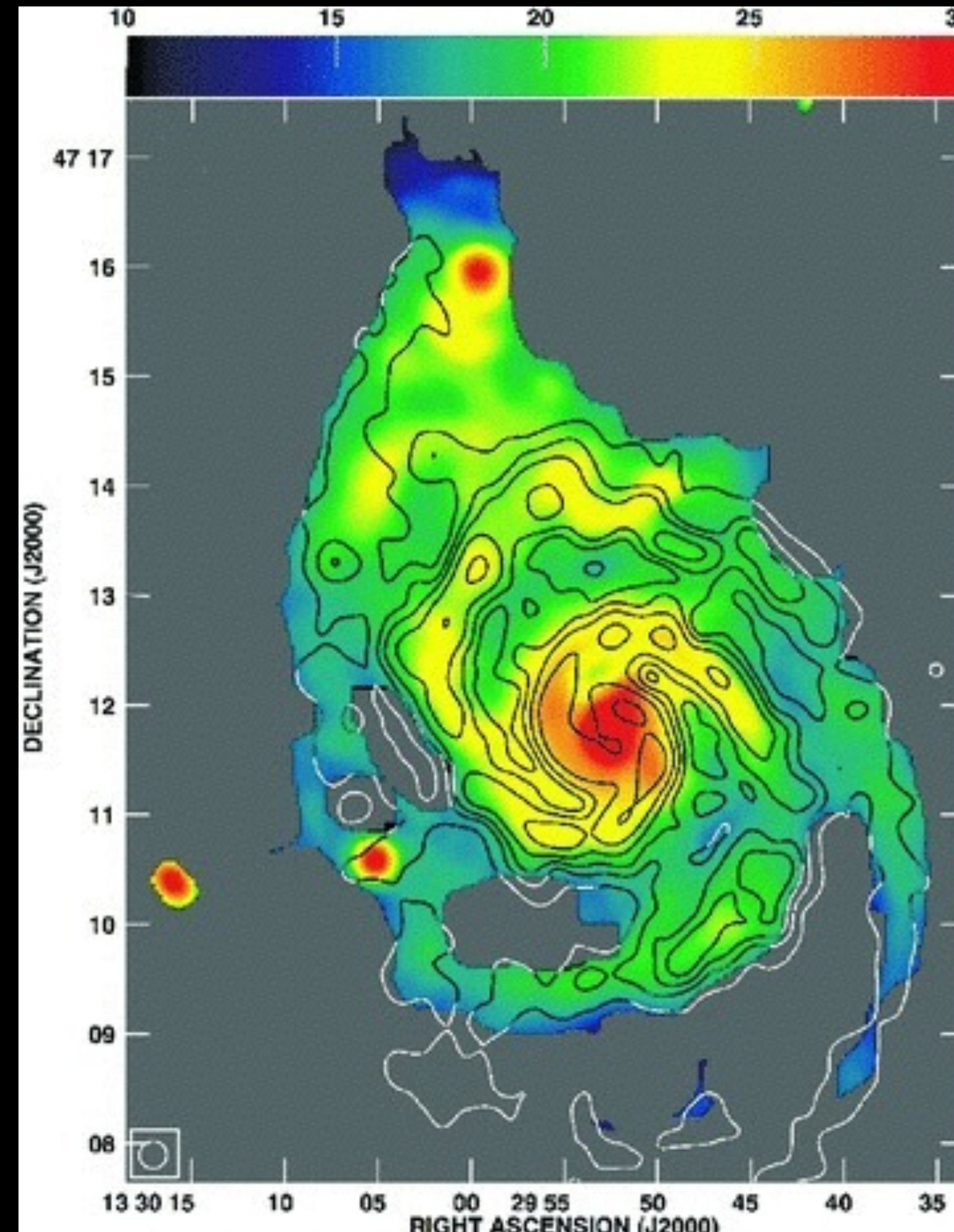

Field strength estimated by assuming energy equipartition with non-thermal synchrotron-emitting electrons

Fletcher+11

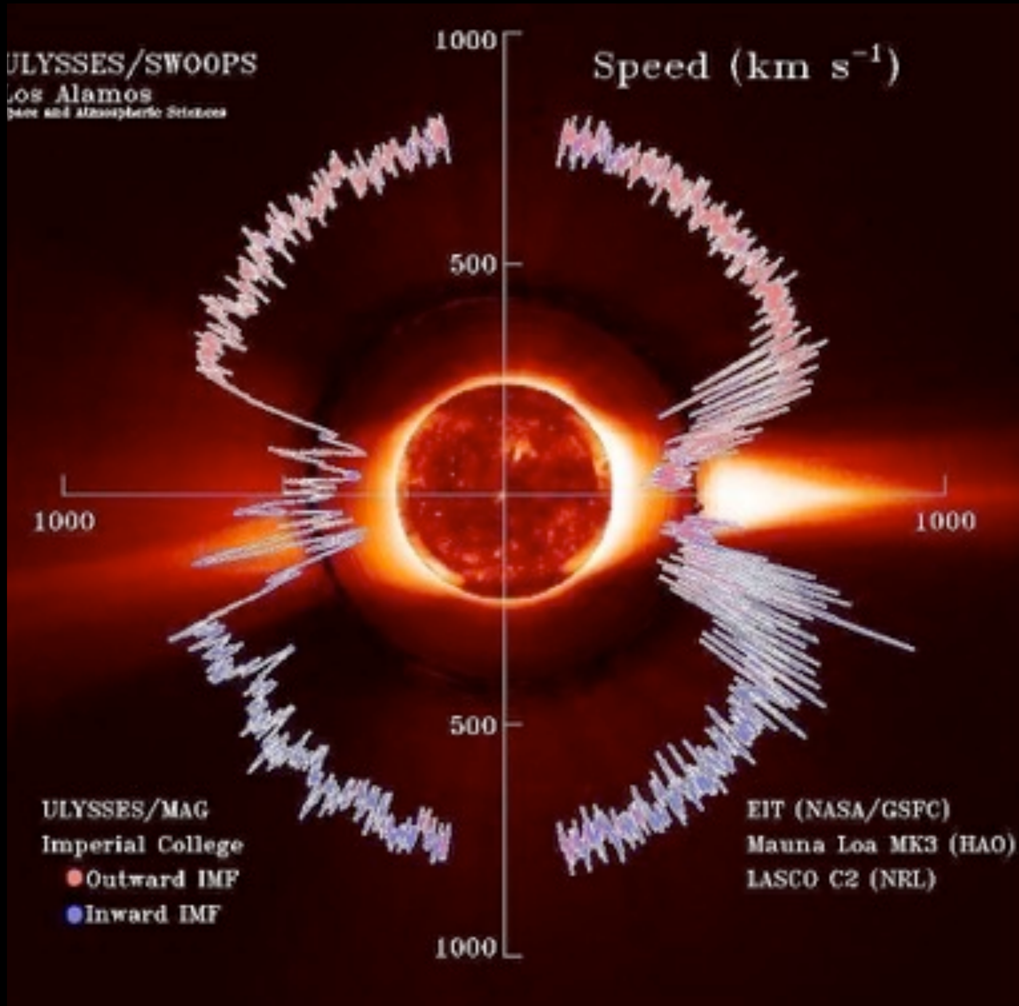

We suppose that the field at the coronal base has an energy density greater than the thermal energy density, so that an initially subsonic flow will follow the field-lines. Gas starting at sufficiently low latitudes will reach the equator at points not too far from the star, where the magnetic energy density is still larger than the thermal. Even if there were no hot gas outside the region defined by the loop ABA' in Fig. 1, exerting an inward pressure, the gas within ABA' would reach equilibrium: a very slight denting of the field-lines would generate the discontinuity in the magnetic pressure $\mathbf{H}^2/8\pi$ that would balance the discontinuity in thermal pressure. But gas expanding along field lines such as EC cannot reach such a state of hydrostatic equilibrium. Before it has expanded far enough to reach the equator, it will find that its pressure exceeds the magnetic pressure, so that it will cease to flow along prescribed, nearly dipole field-lines: instead it will expand more-or-less radially, dragging the field with it.

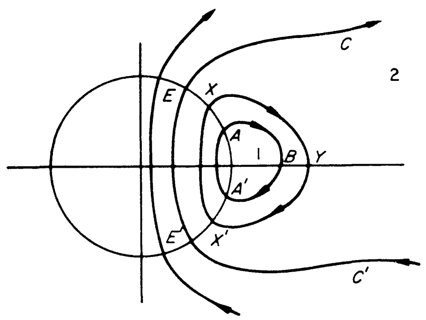

FIG. 1

Mestel 65

The picture we arrive at finally is as in Fig. 1. There is a dead zone (1) in which the closed, approximately dipolar field-loops hold in the gas and keep it rotating with the star's angular velocity Ω_s. The density field ρ along each field-line is given by the component of hydrostatic support along the field: assuming isothermality with sound speed a,

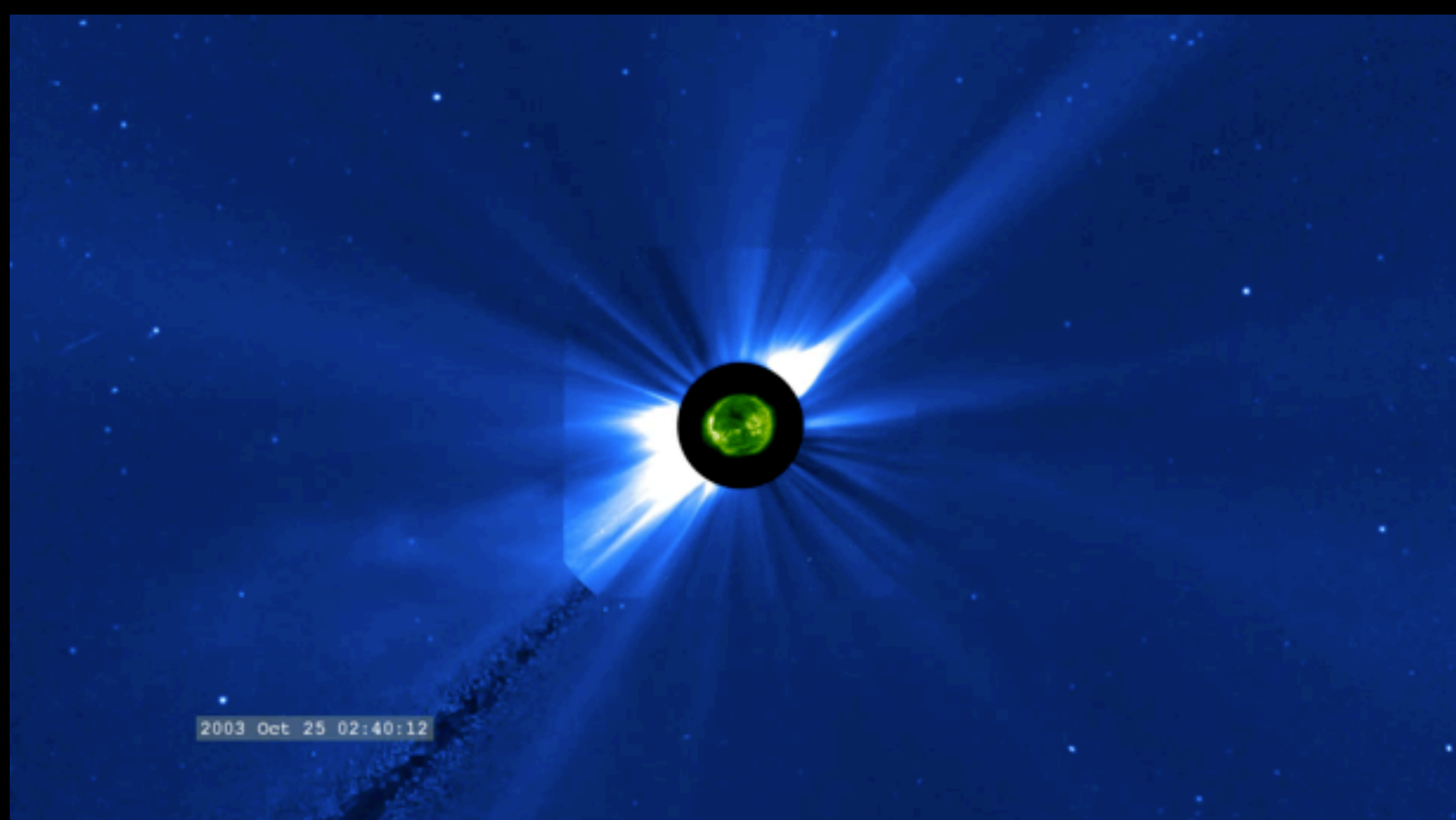

“Pulsar wind nebula” in Crab Nebula

1 pc

MHD model

- Acceleration
  - Magneto-centrifugal force (Blandford-Payne 1982)
    - Like a force worked a bead when swing a wire with a bead
  - Magnetic pressure force
    - Like a force when stretch a spring
  - Direct extract a energy from a rotating black hole
- Collimation
  - Magnetic pinch (hoop stress)
    - Like a force when the shrink a rubber band

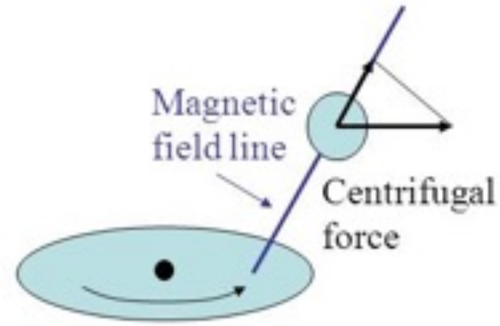

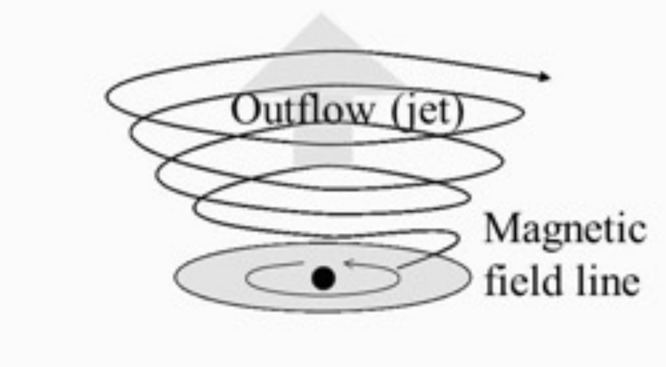

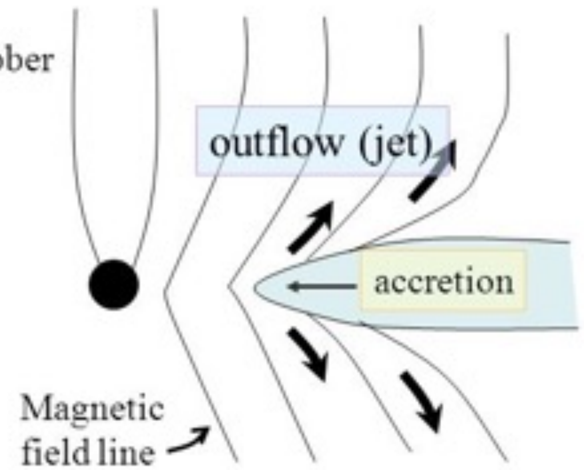

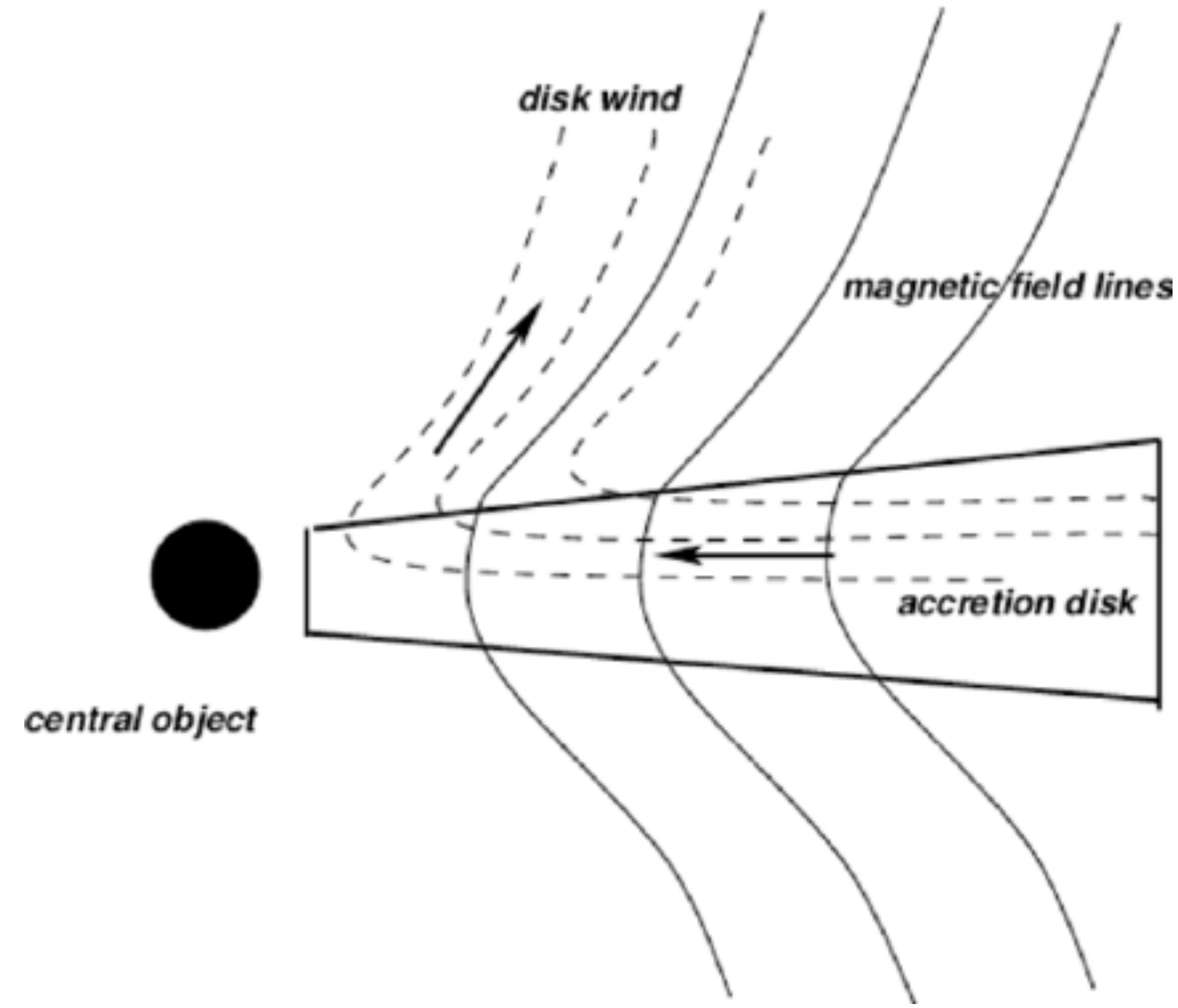

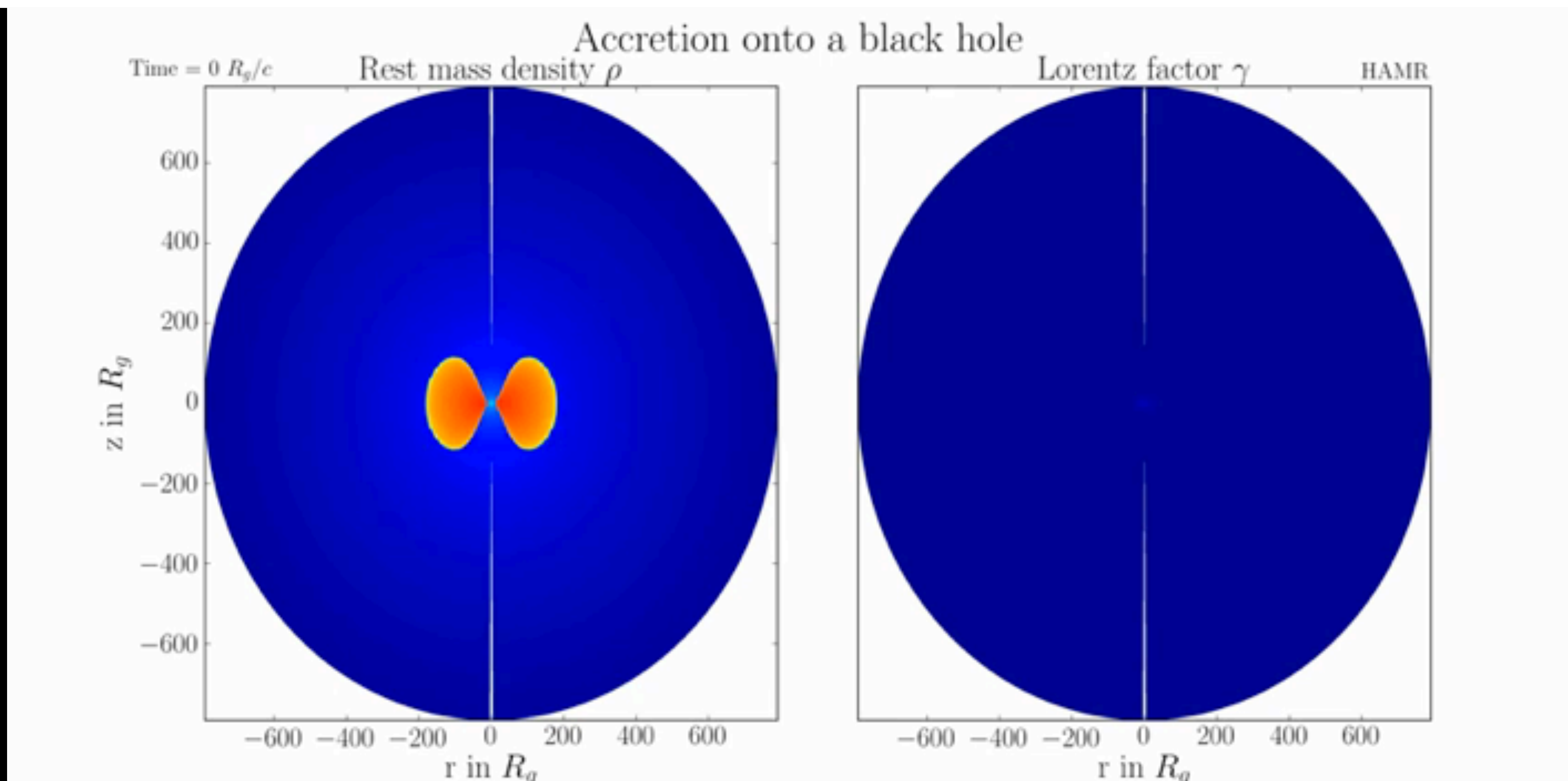

Hesp, Liska, Tchekhovskoy

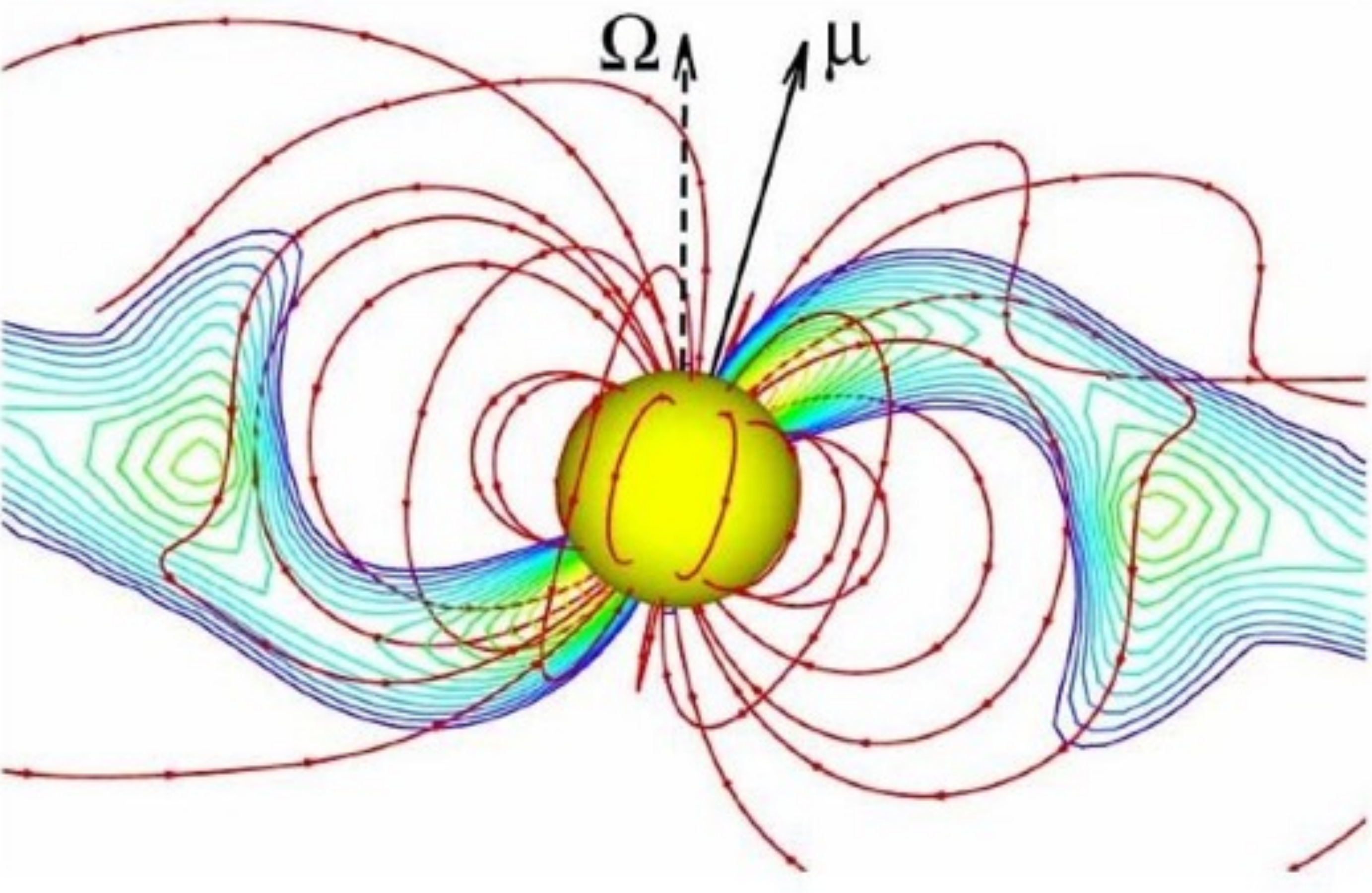
Ω
μ

Magneto-rotational instability (MRI) / Hawley & Balbus 91

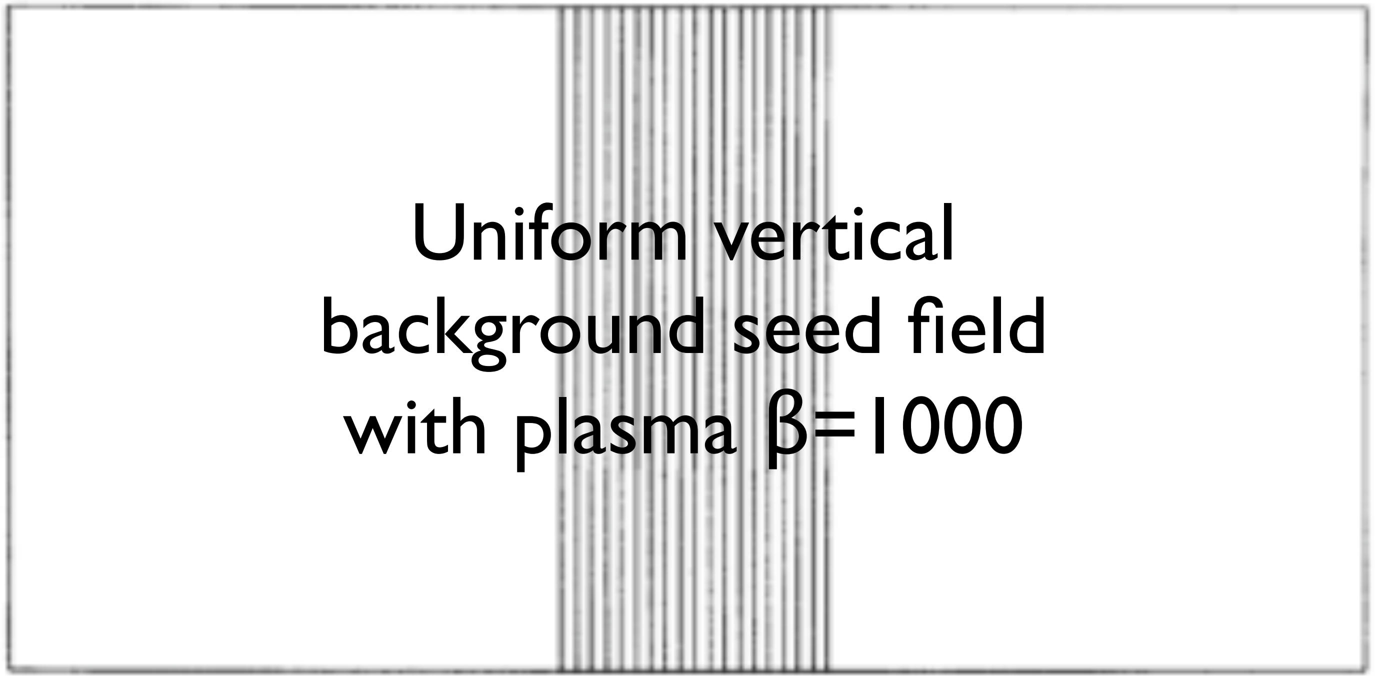

FIG. 3a

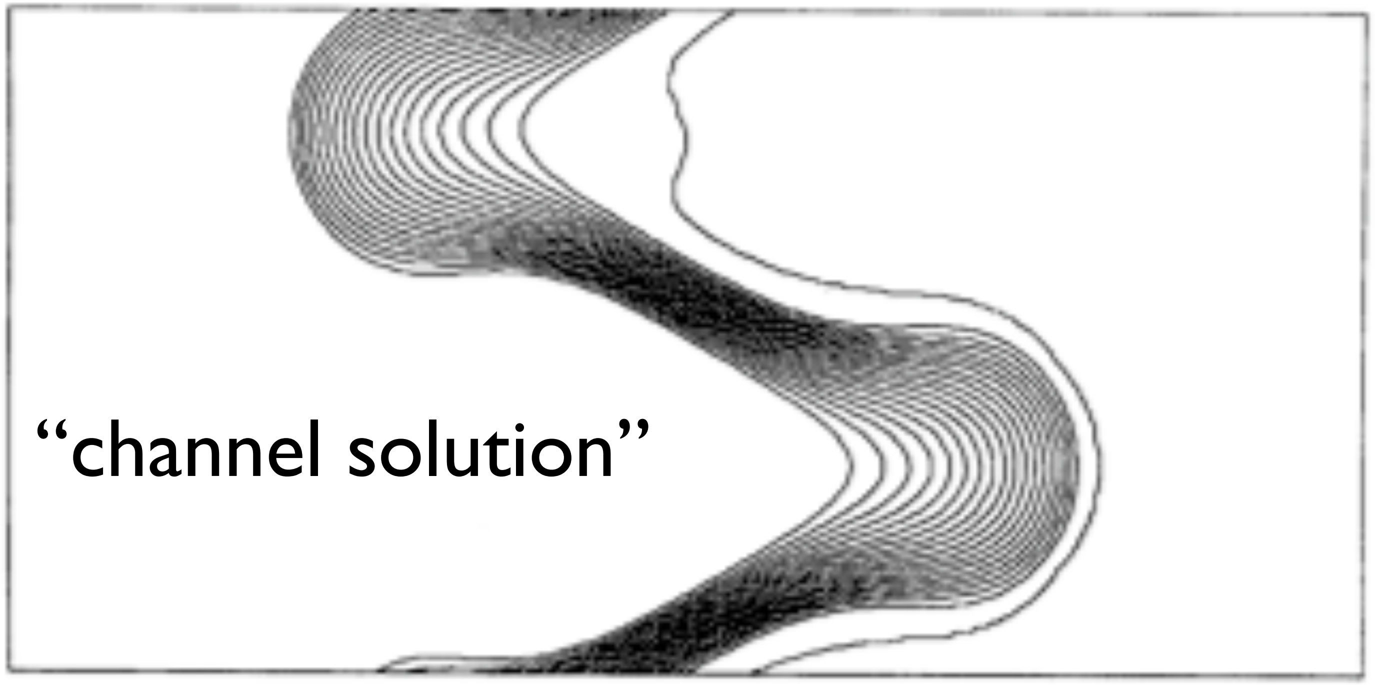

FIG. 3b

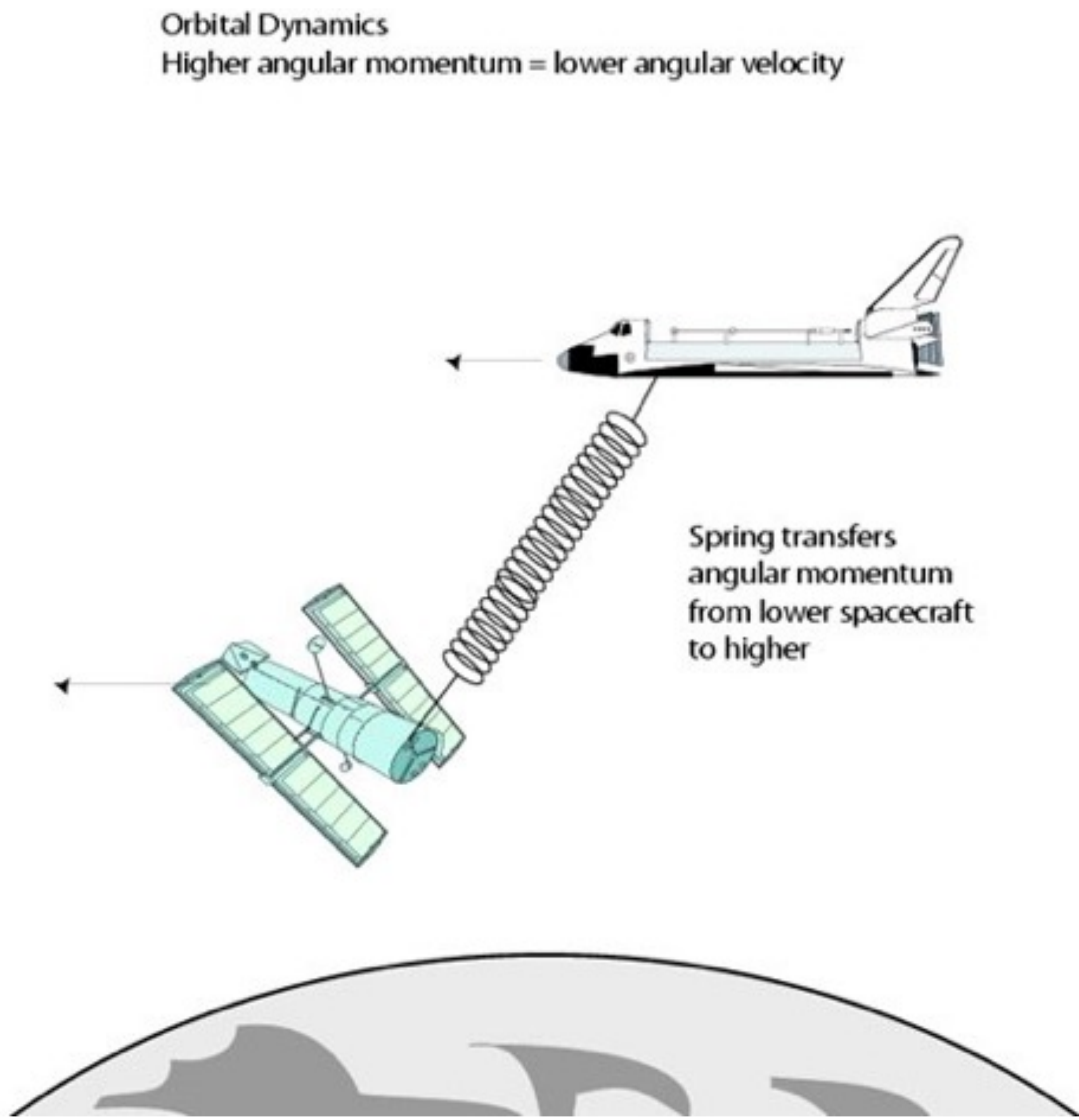

MRI accretion

- Turbulence and transport are consequences of differential rotation and magnetism

- The MRI is an effective dynamo: amplifies B and even produces magnetic cycles (like on the Sun)

- The flow is *turbulent,* not viscous.
  Turbulence is a property of the flow;
  viscosity is a property of the fluid.

- An MRI-turbulent disk and a viscous accretion disk having the same total alpha behave differently, especially in 3D

Hawley 2000

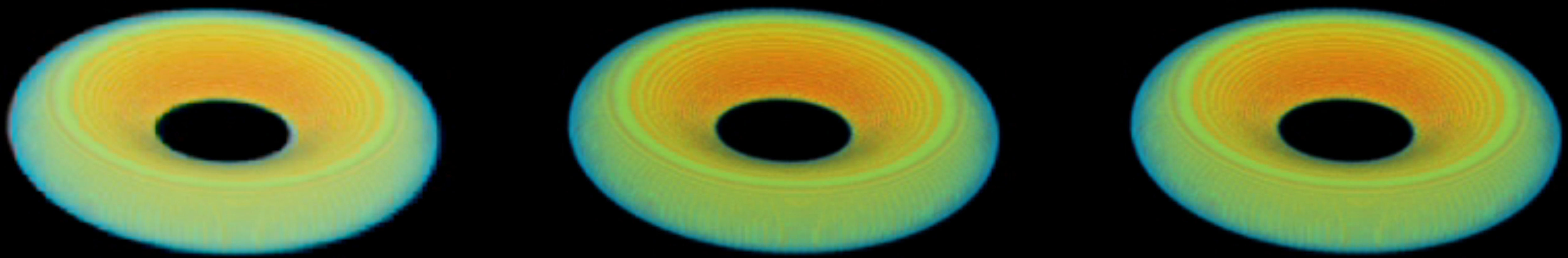

Hawley 2000

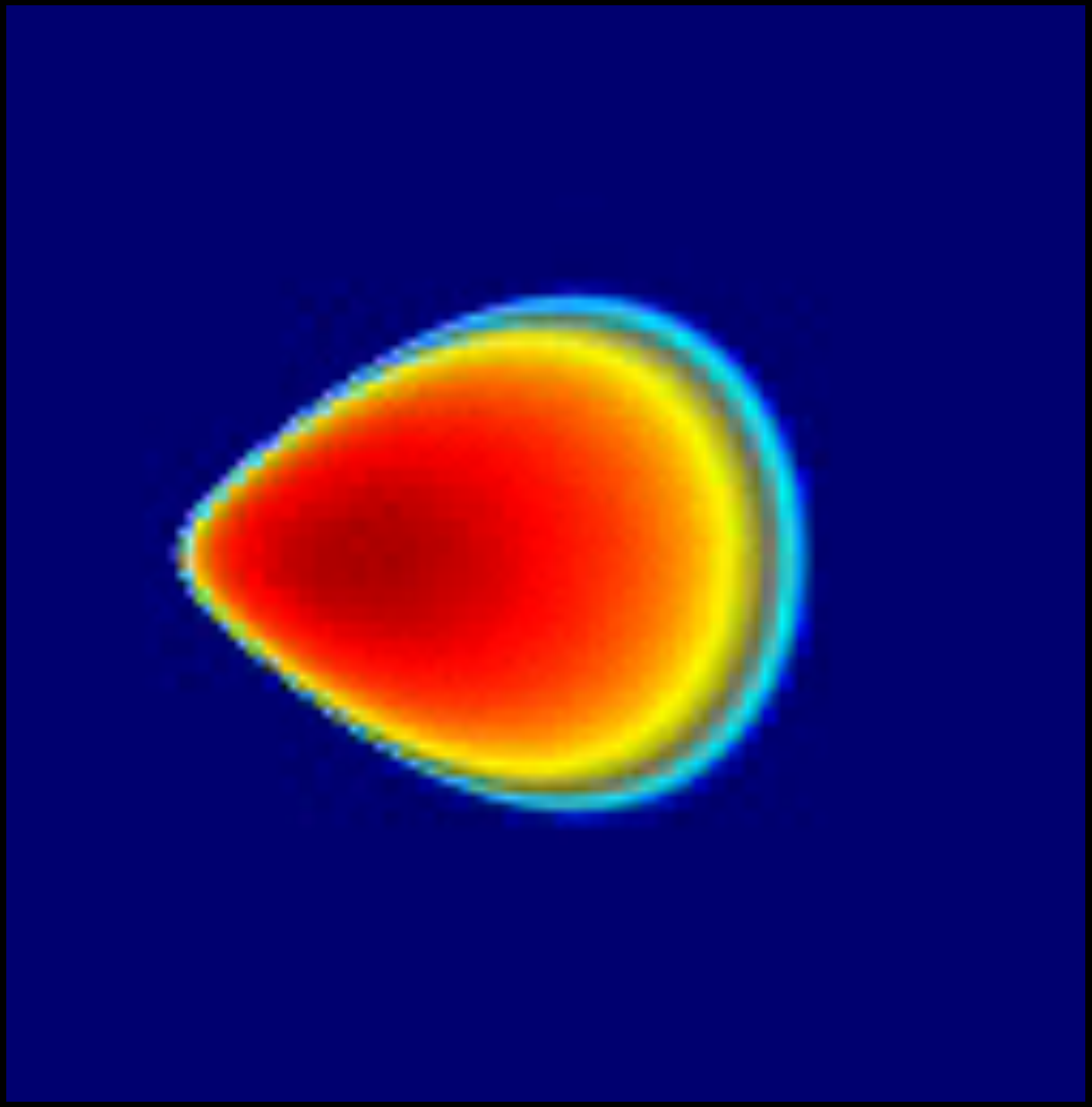

3-D

Colors denote log density

Initially poloidal field

Hawley, Gammie, & Balbus 95

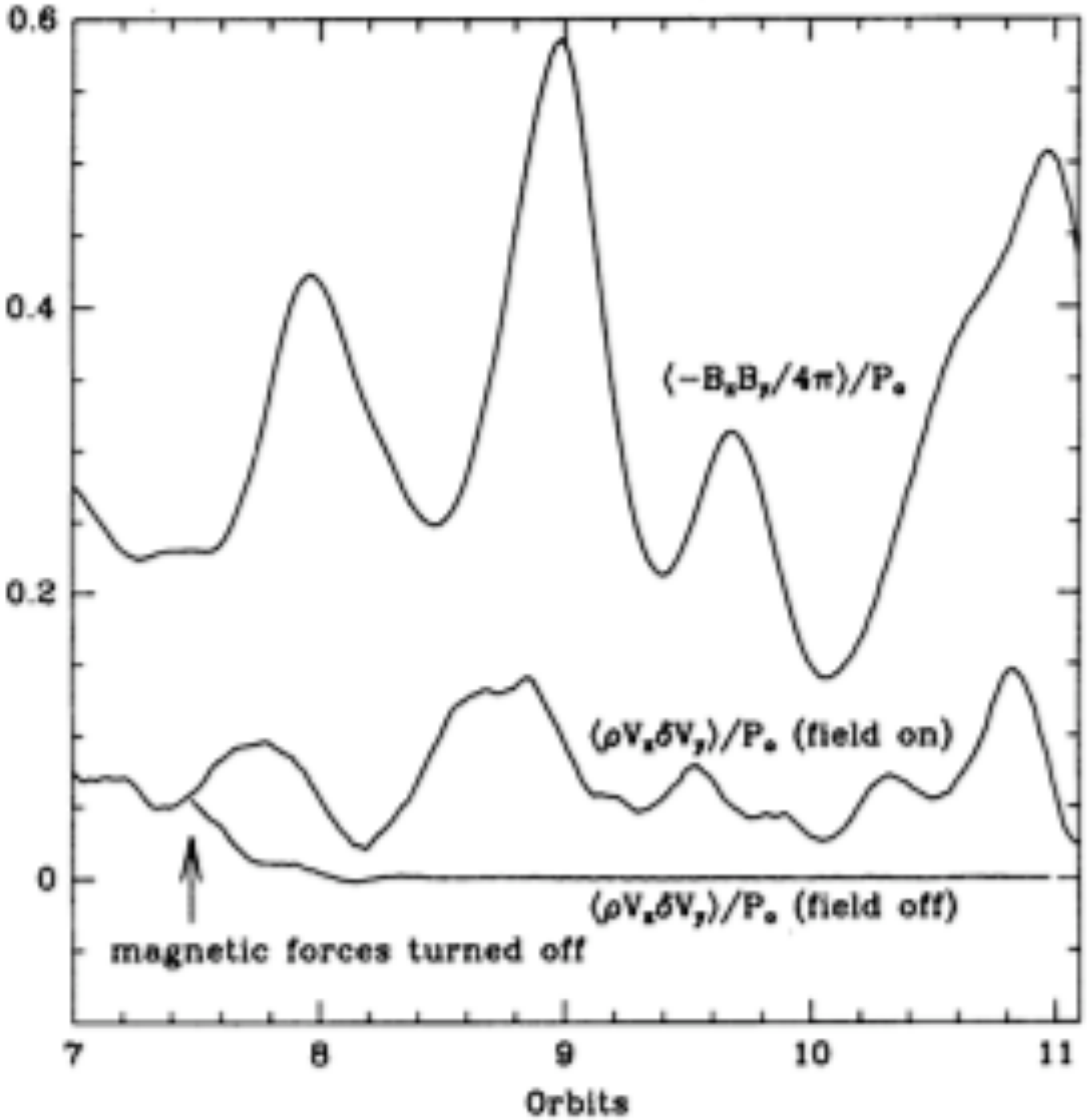

FIG. 7.—The Maxwell and Reynolds stresses in the fiducial run Z4 compared with the Reynolds stress seen in a purely hydrodynamical simulation that is initialized with data from model Z4 at time $t = 7.5$. Without magnetic fields the net Reynolds stress vanishes within one orbit. The time series are boxcar smoothed on a timescale of 0.25 orbits.

Uniform vertical background seed field with plasma β=400

Bai & Stone 13a

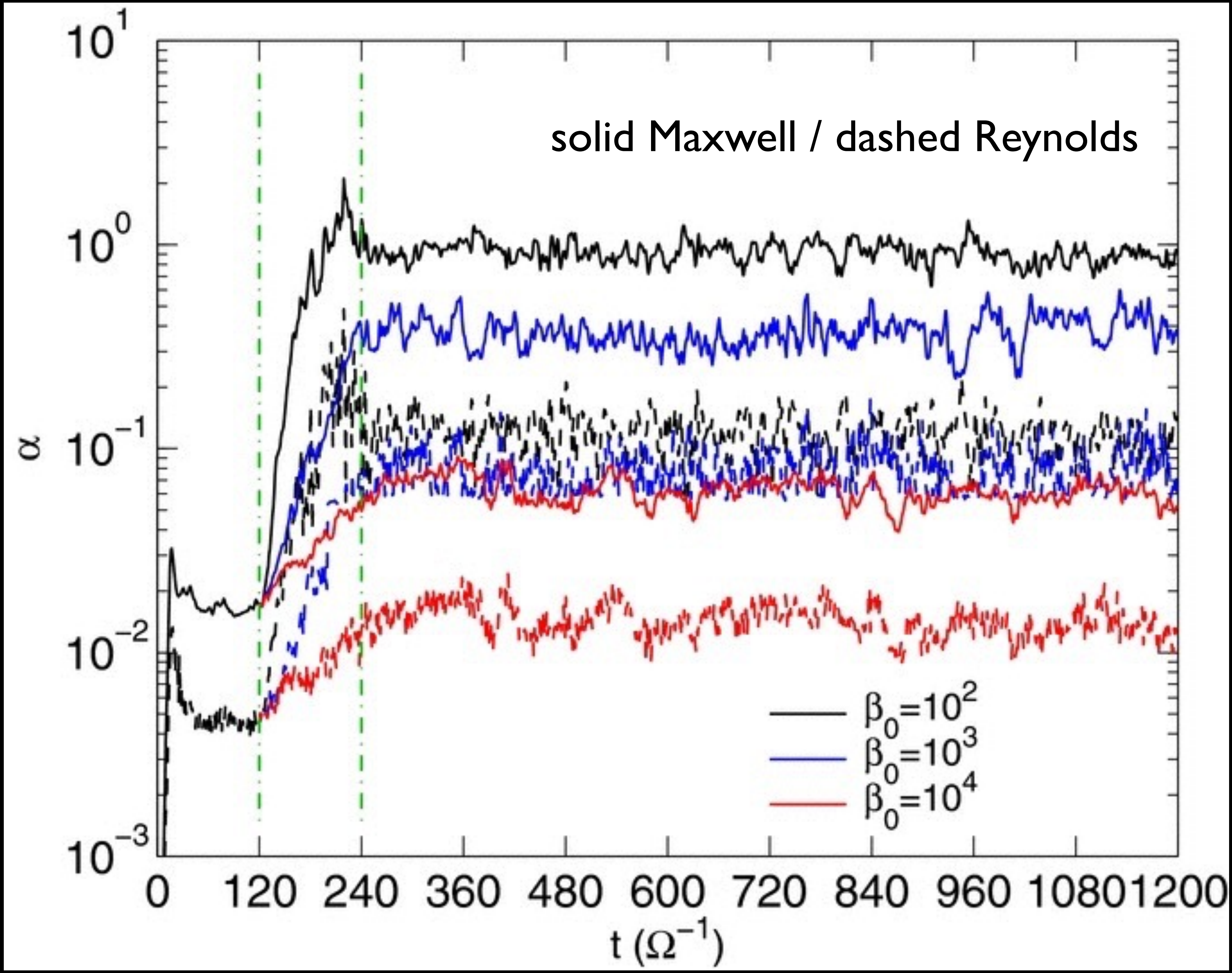

uniform net vertical B_0

Bai & Stone 13a

MRI as dynamo: Generation of enormous and cyclical toroidal B_φ

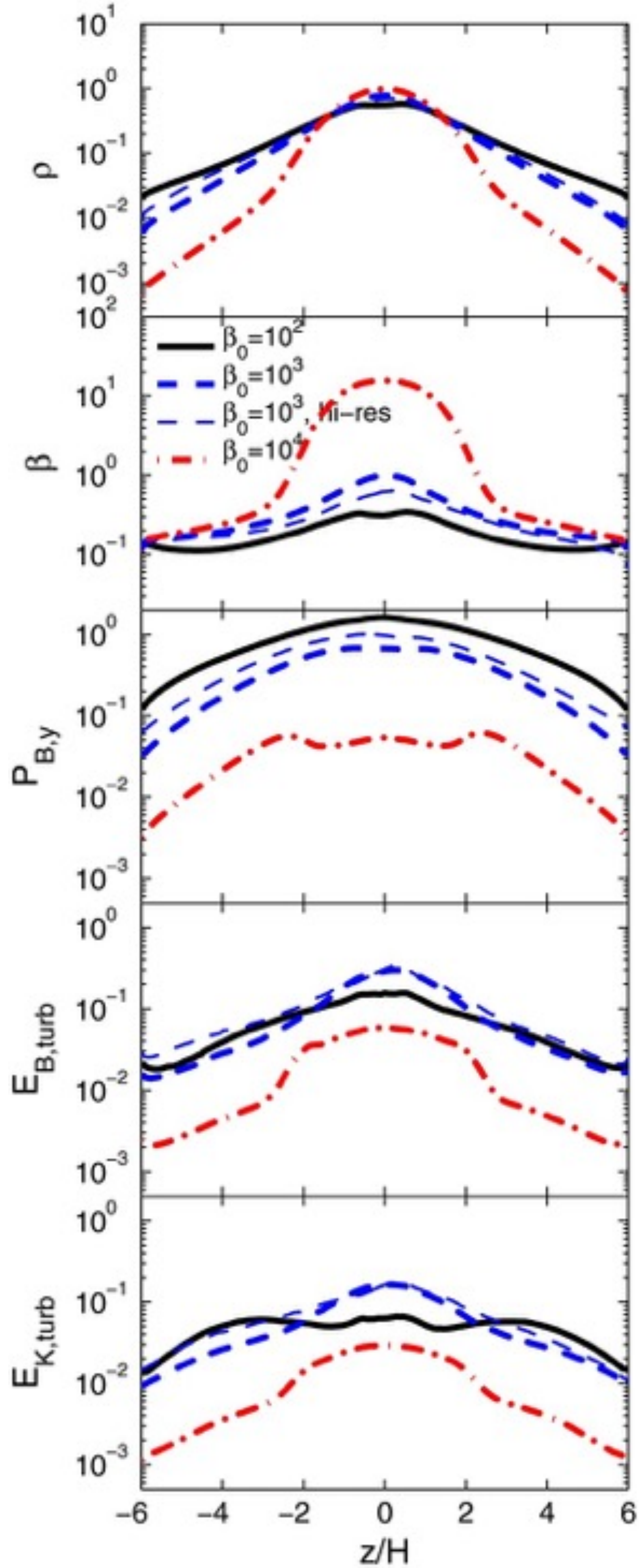

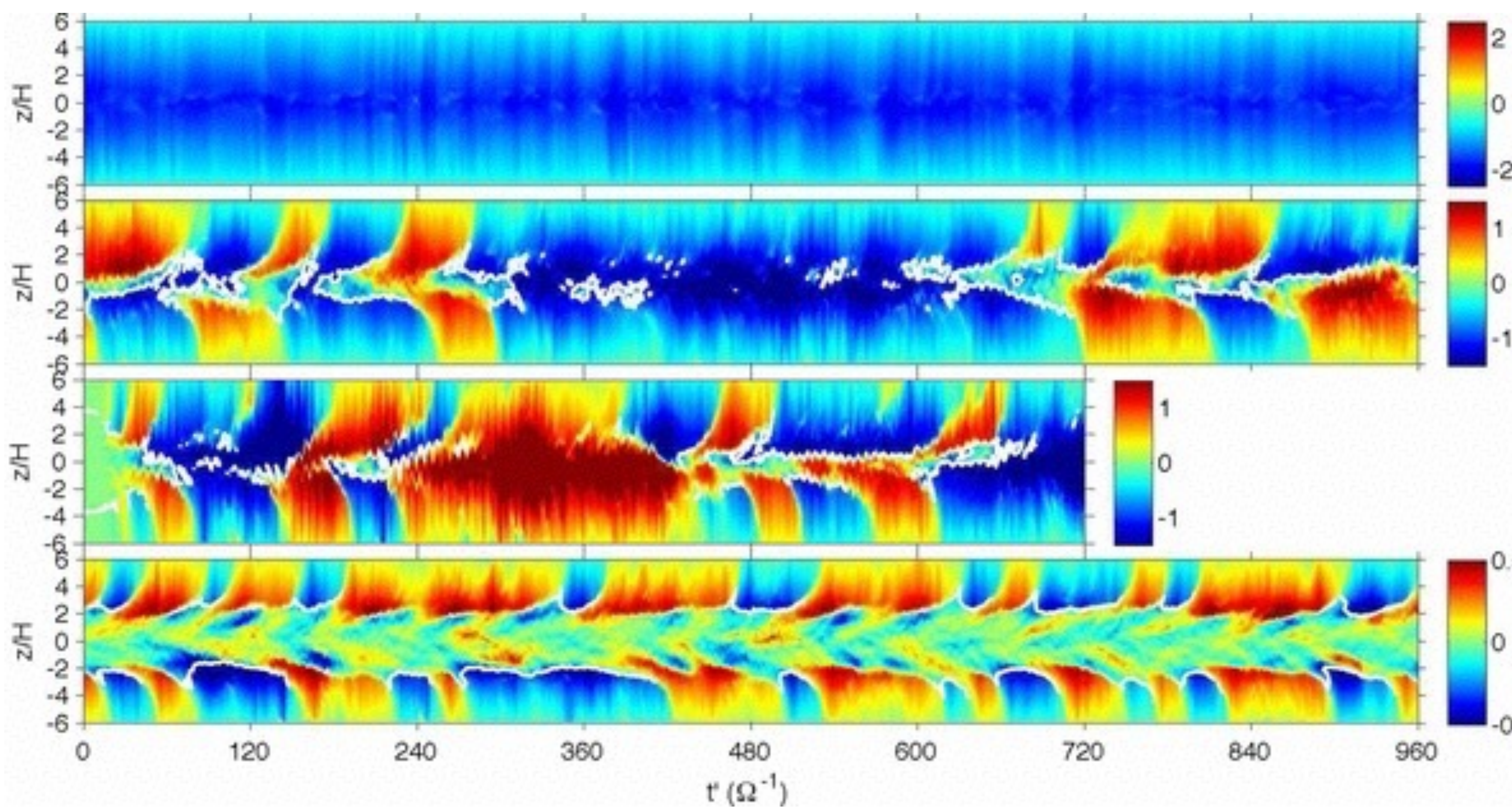

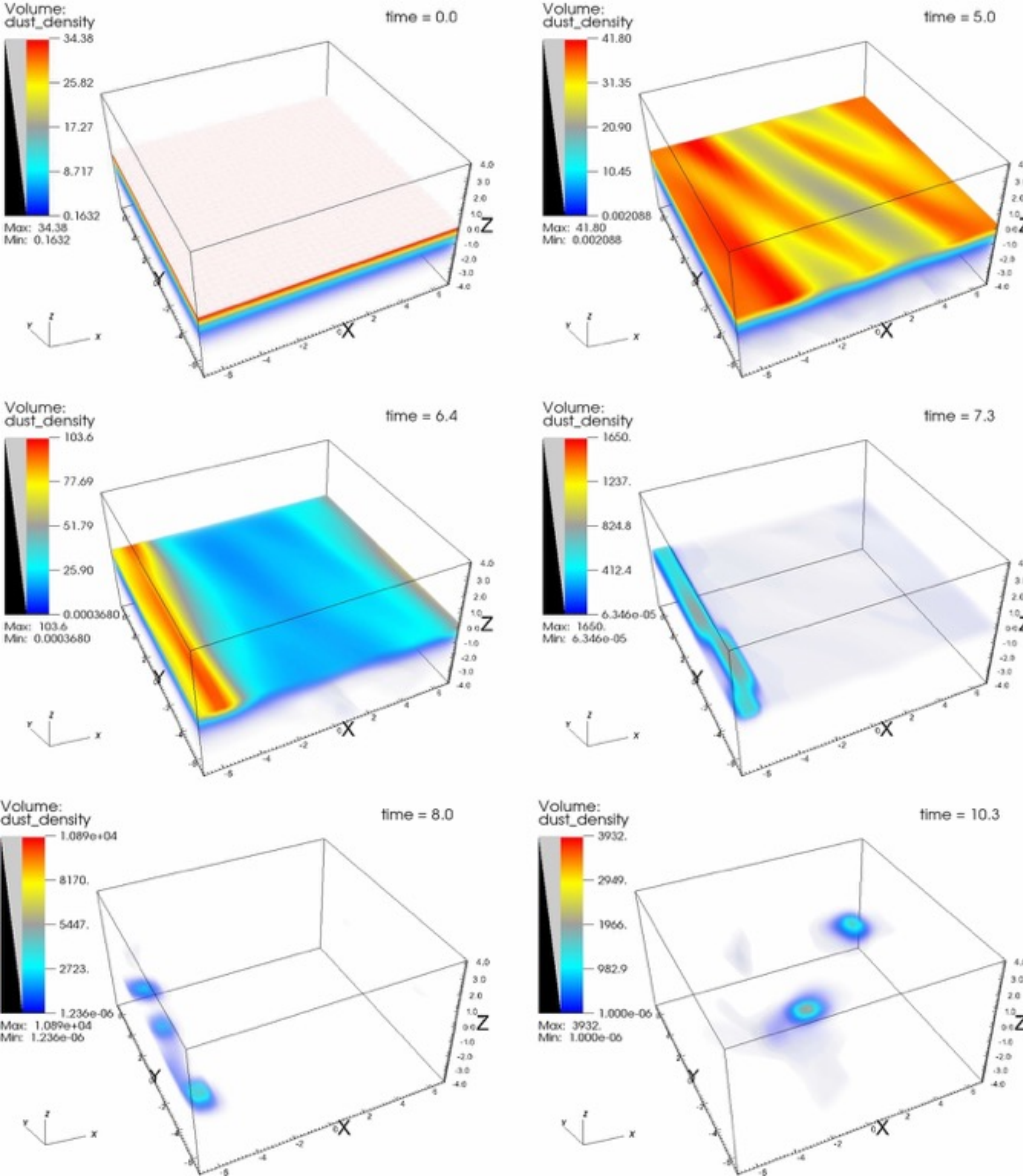

$$t_{\rm cool} < t_{\rm shear} \sim t_{\rm orbit}$$

Q ~ 1 but fast cooling:
gravitational collapse

Shi & Chiang 13

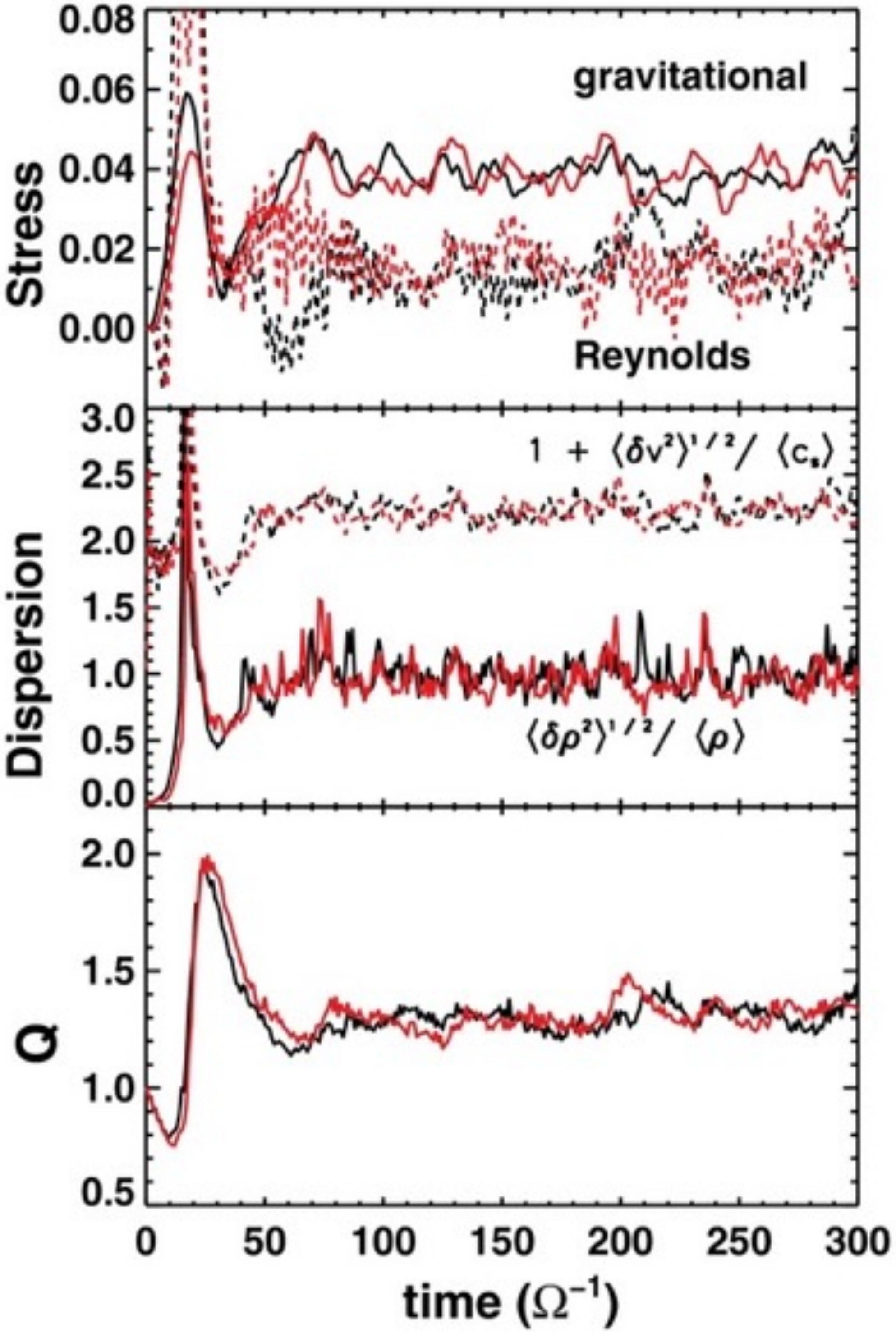

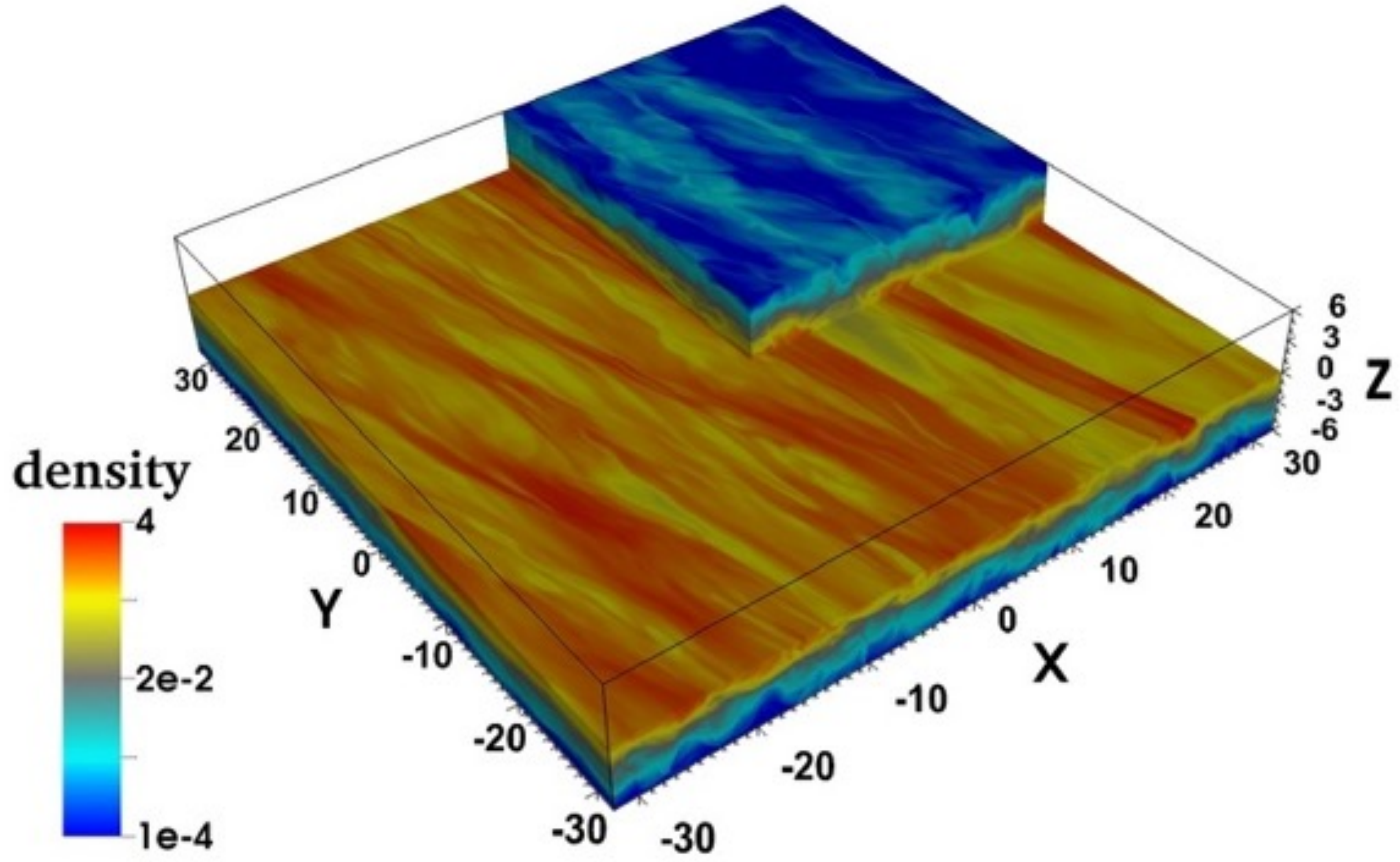

Shi & Chiang 14

$$t_{\rm cool} > t_{\rm shear} \sim t_{\rm orbit}$$

Q ~ 1 but long cooling: "gravito-turbulent"

How do disks accrete?

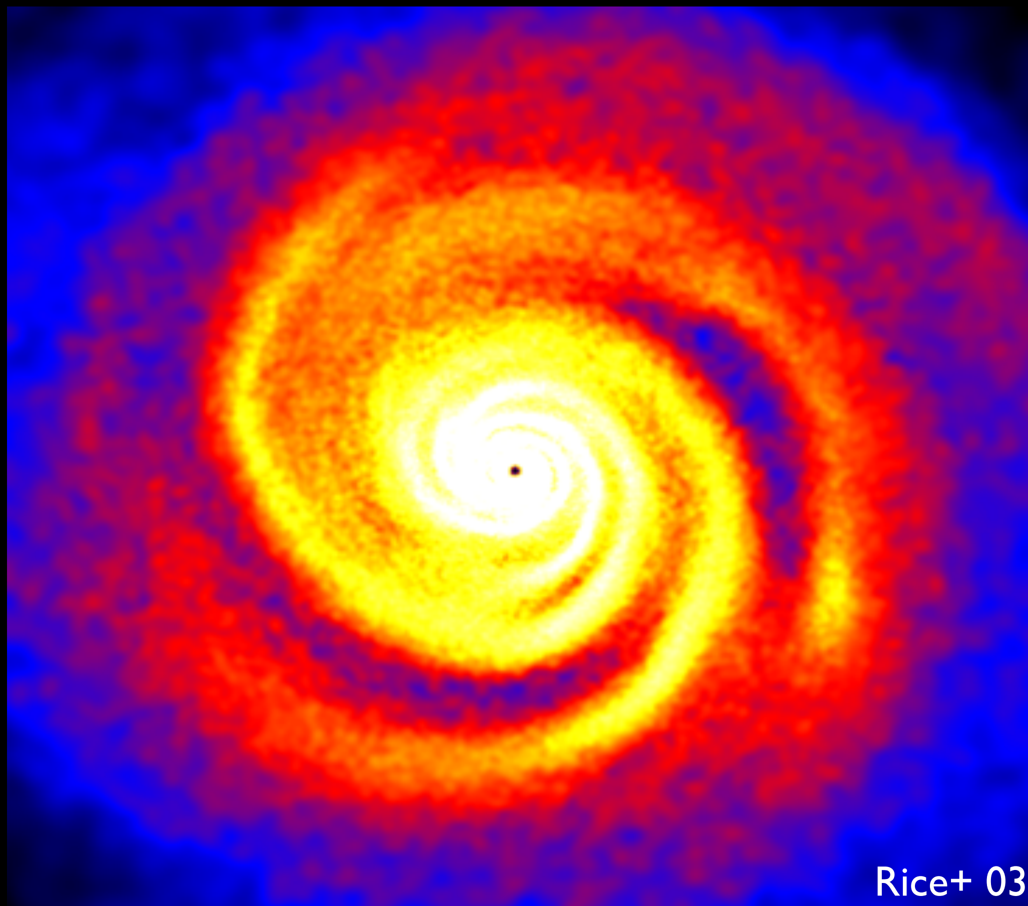

Spiral features revealed in SAO 206462's dust disk

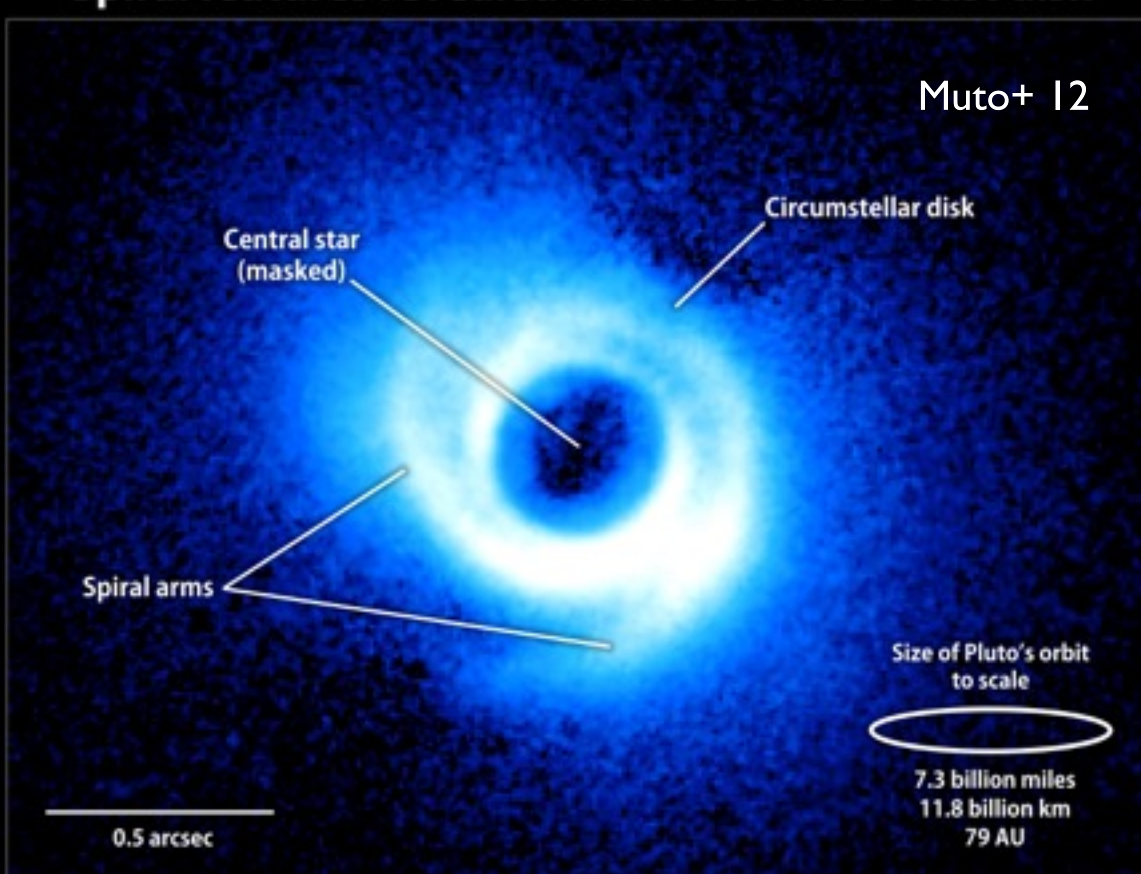

Gravitational instability (GI)

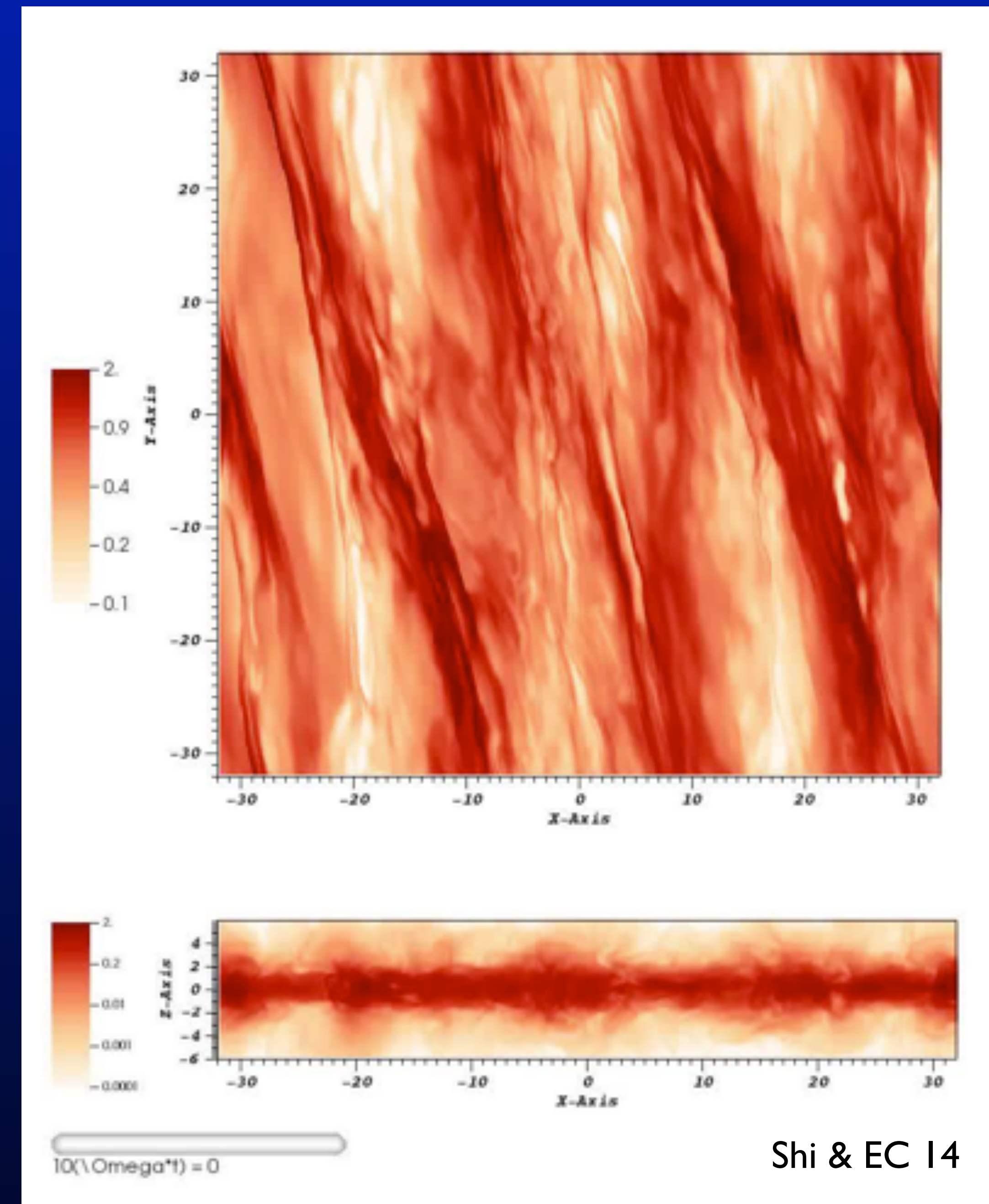

$$Q = \frac{c_s \kappa}{\pi G \Sigma} \sim 1$$

$$\Rightarrow \quad M_{\rm disk} \sim \frac{h}{r} M_*$$

Self-gravitating disks
swing amplify
perturbations
into trailing spirals

Goldreich & Lynden-Bell 63

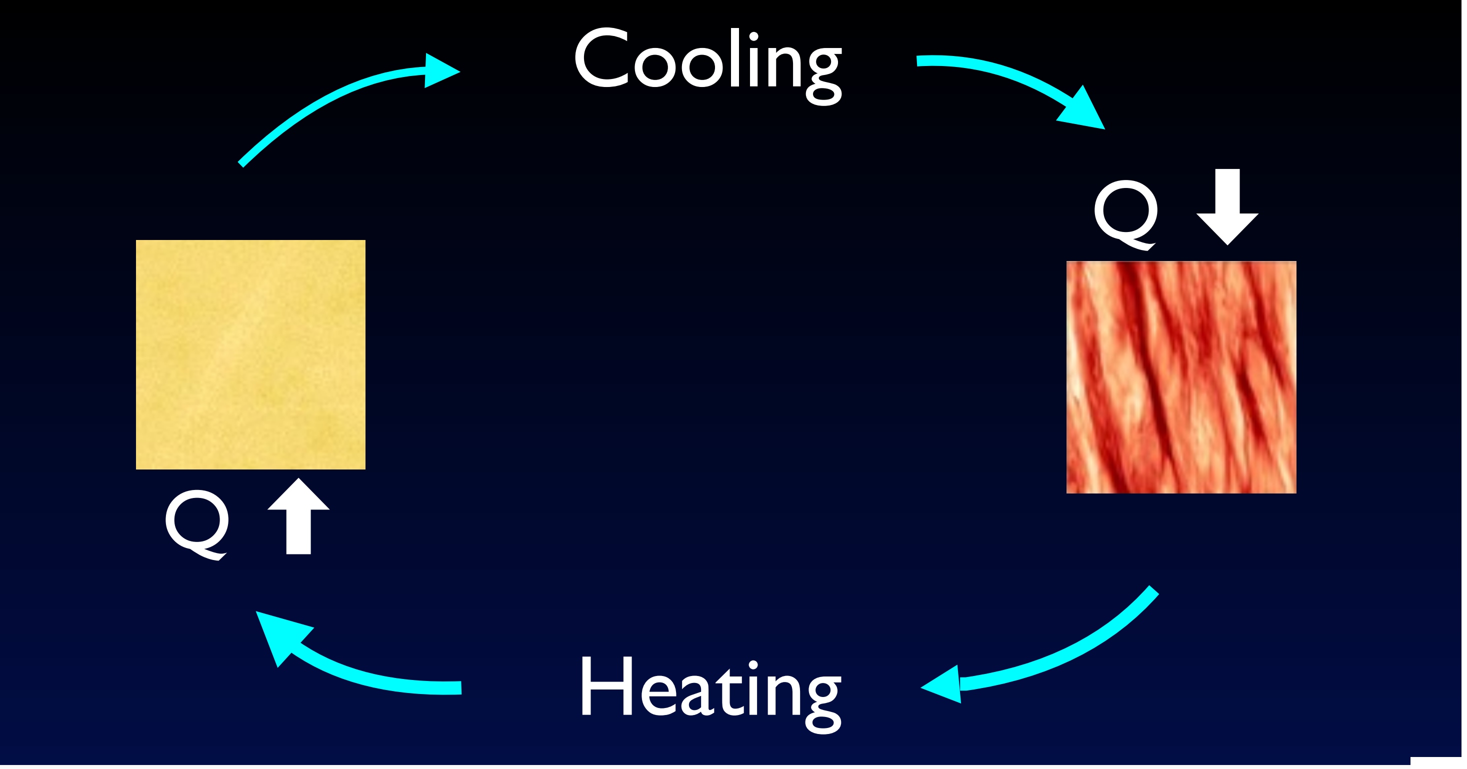
Cooling
Q
Q
Heating

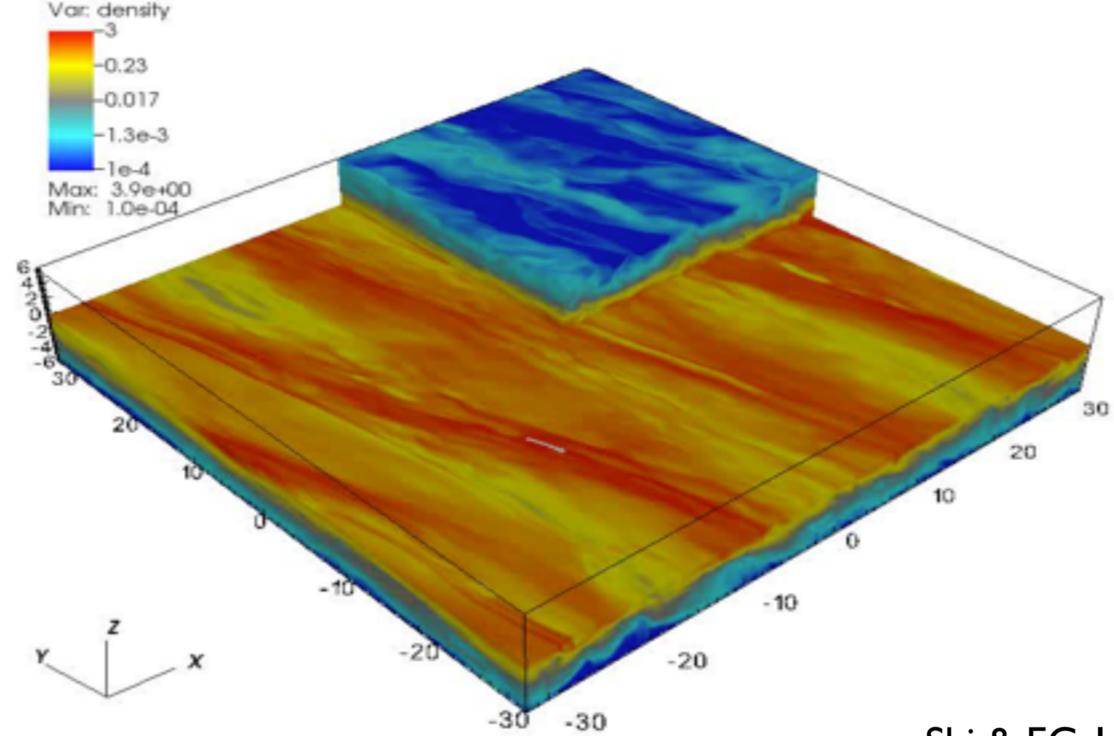
Var: density
Max: 3.9e+00
Min: 1.0e-04

Shi & EC 14

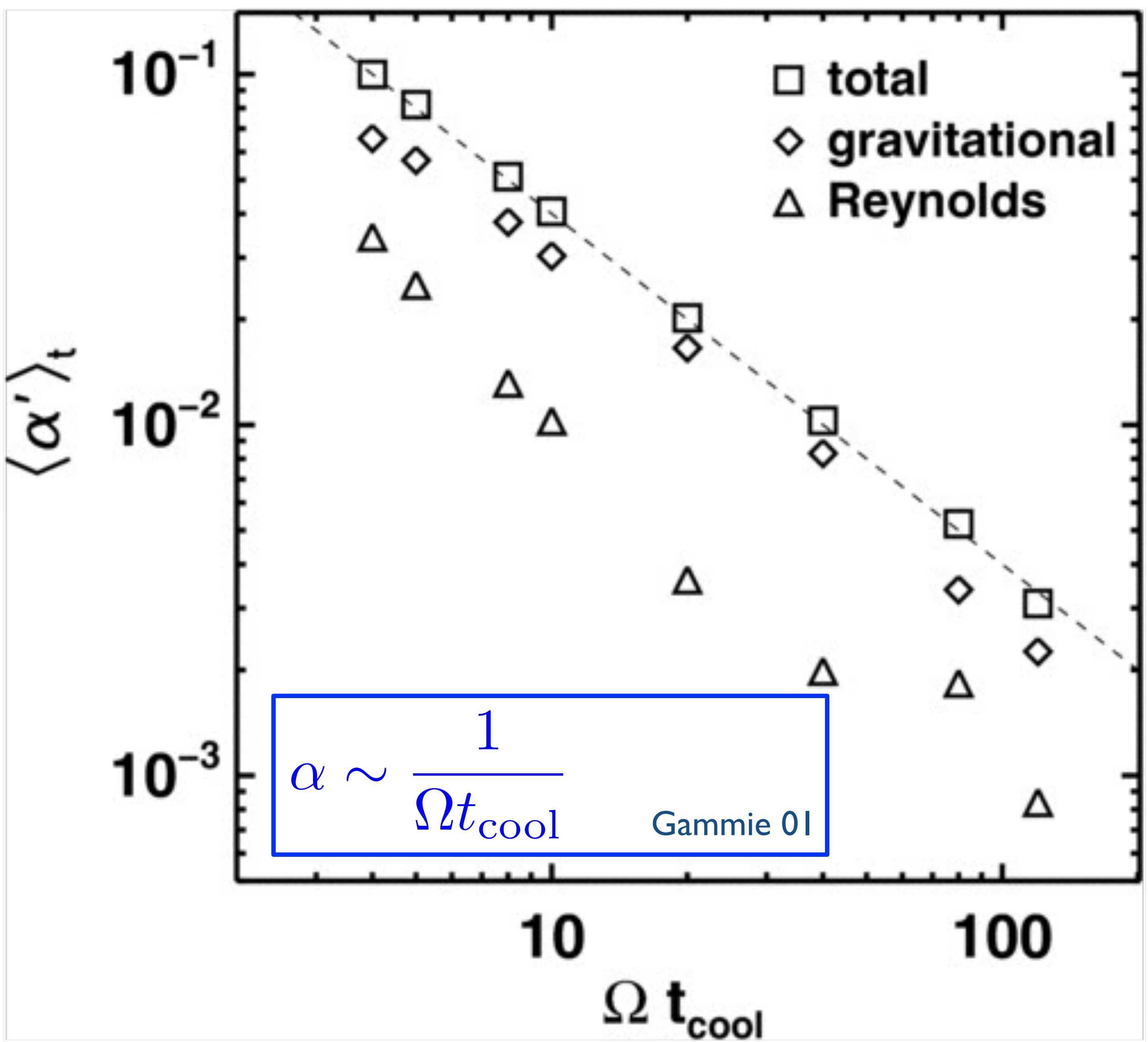
total
gravitational
Reynolds
$\langle \alpha' \rangle_t$
$\Omega\, t_{cool}$
$\alpha \sim \frac{1}{\Omega t_{\rm cool}}$
Gammie 01

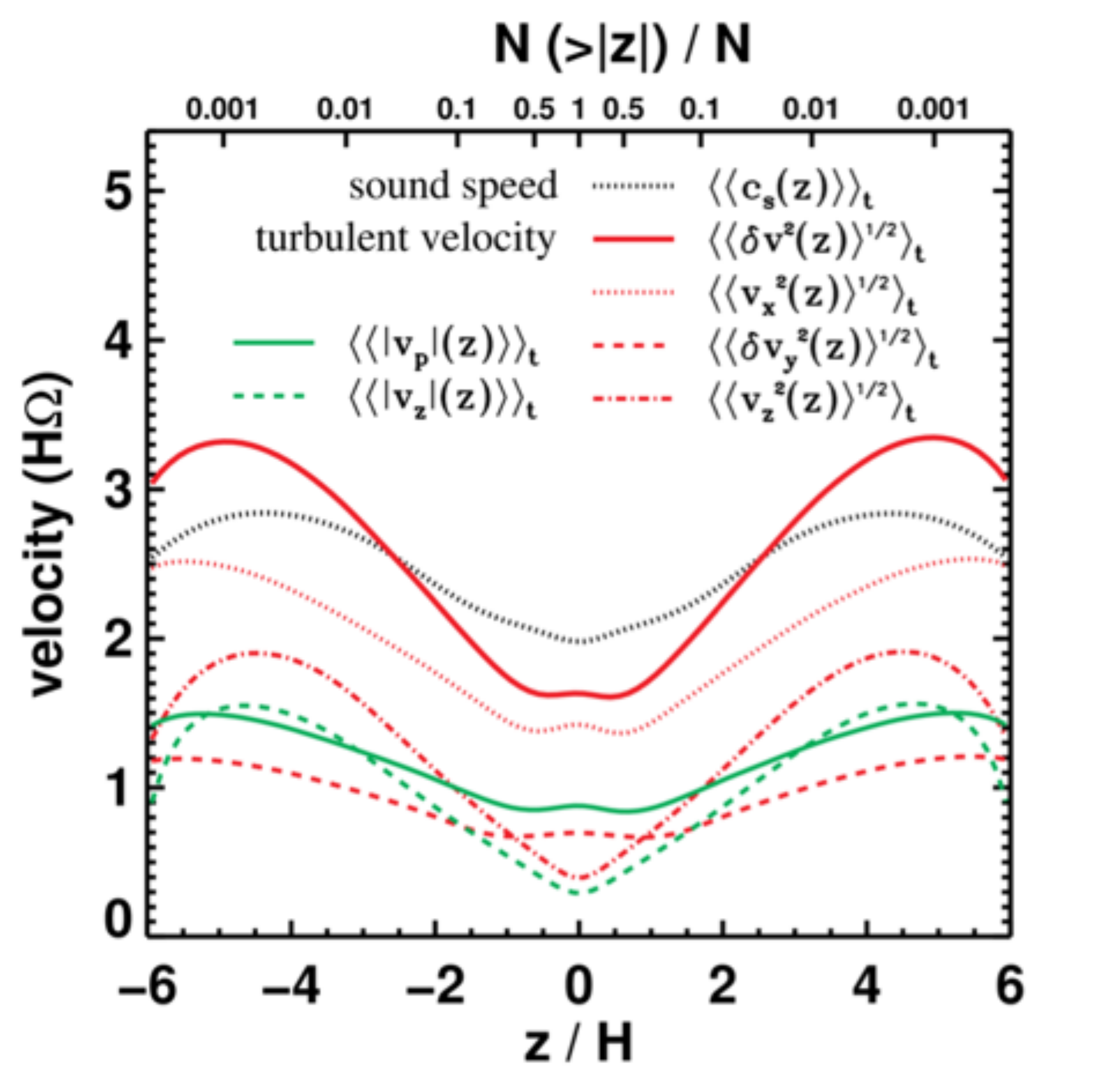
N (>|z|) / N
sound speed
turbulent velocity
velocity (HΩ)
z / H

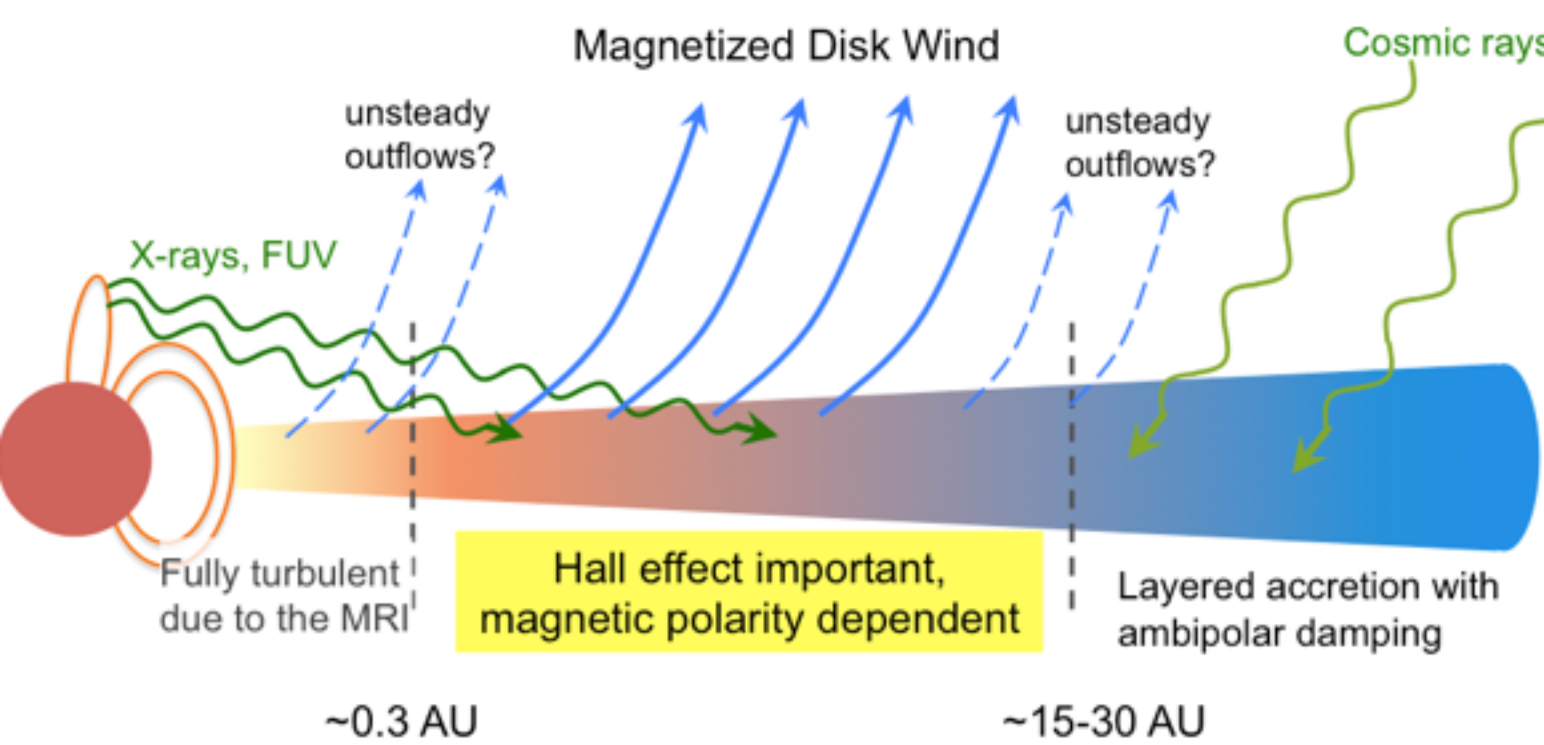

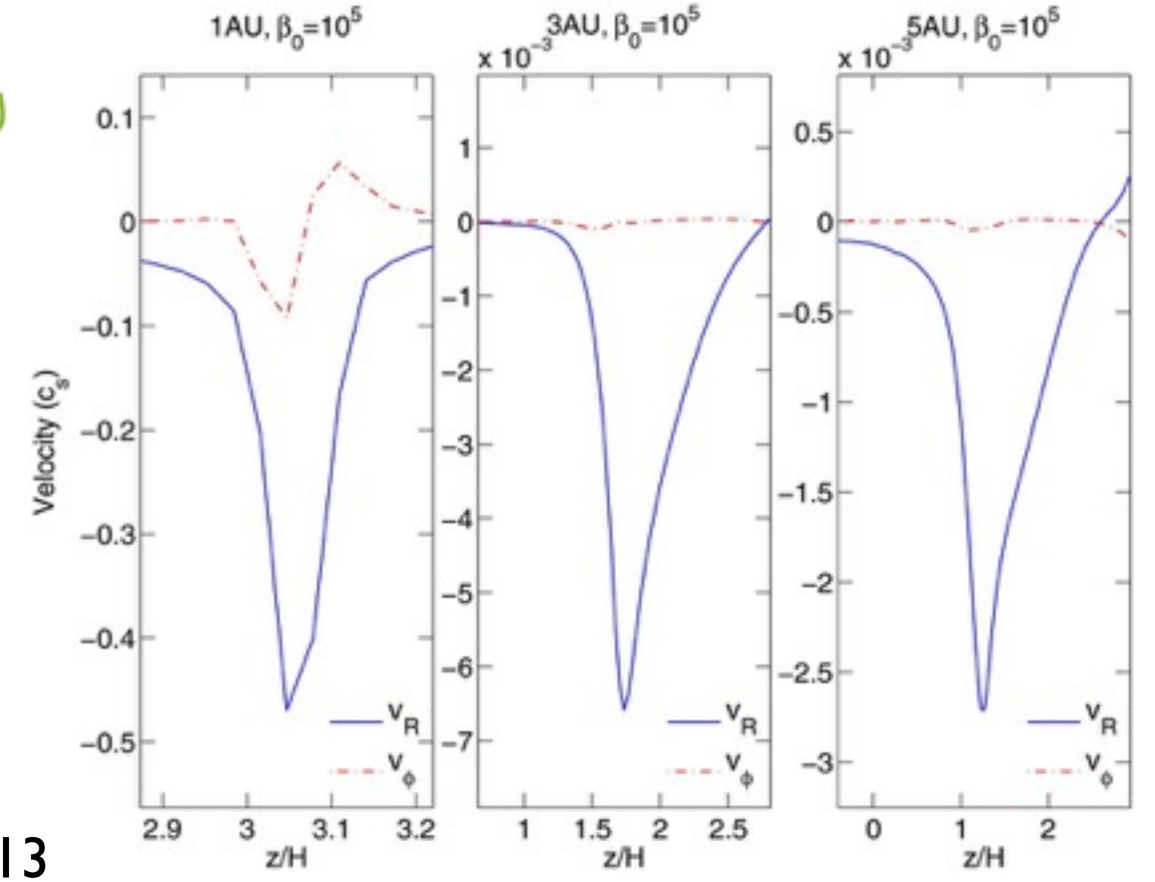

Bai & Stone 13, Bai 13

Protoplanetary disk accretion by surface layer magnetic winds

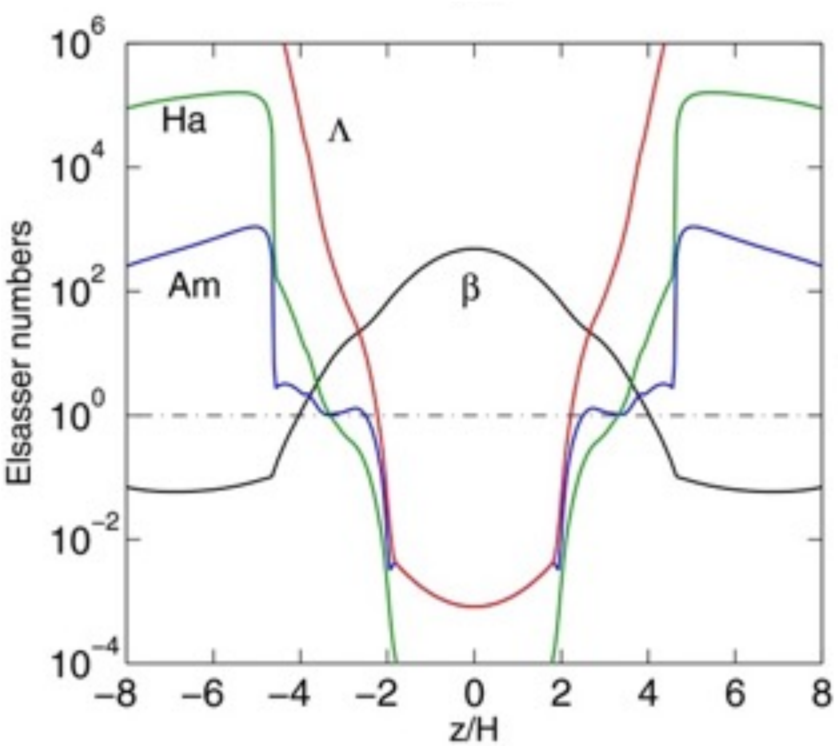

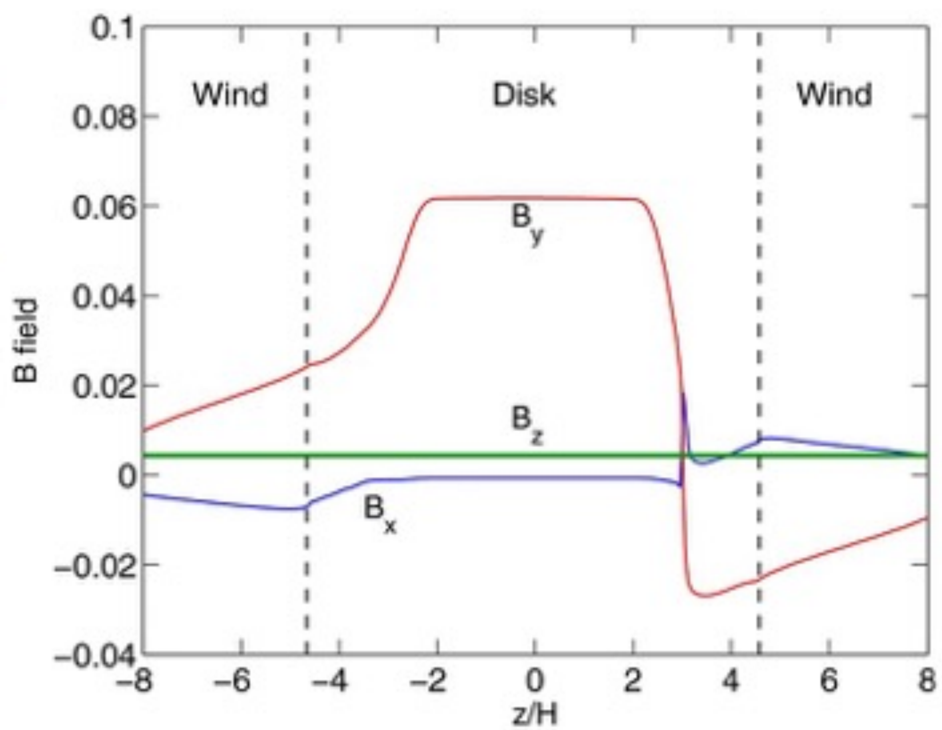

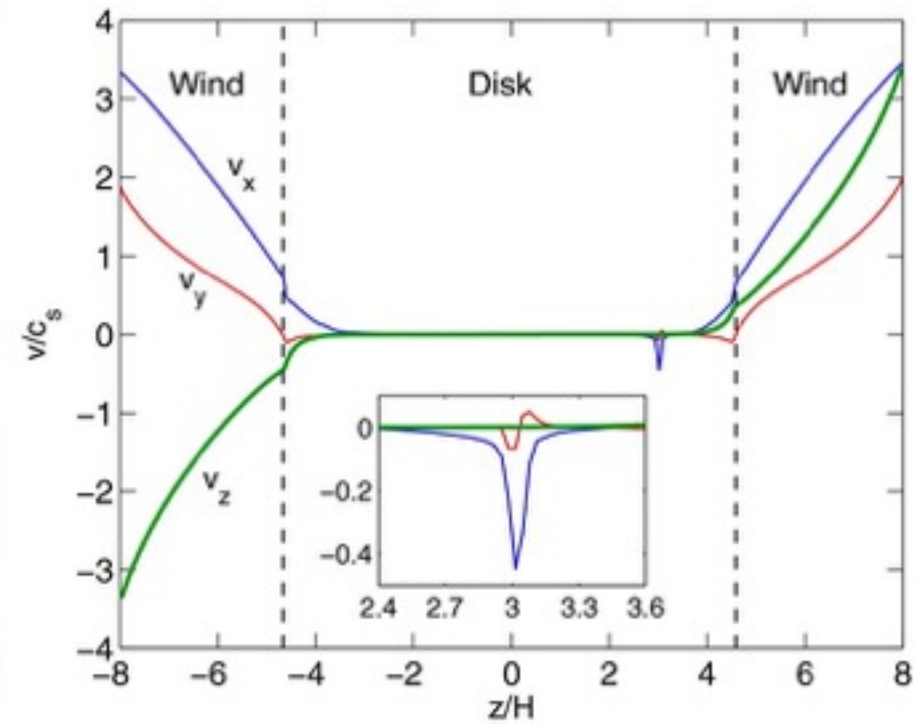

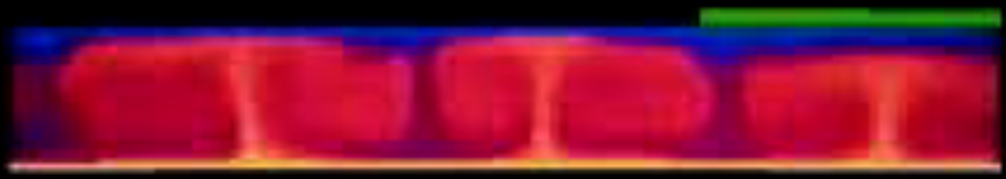

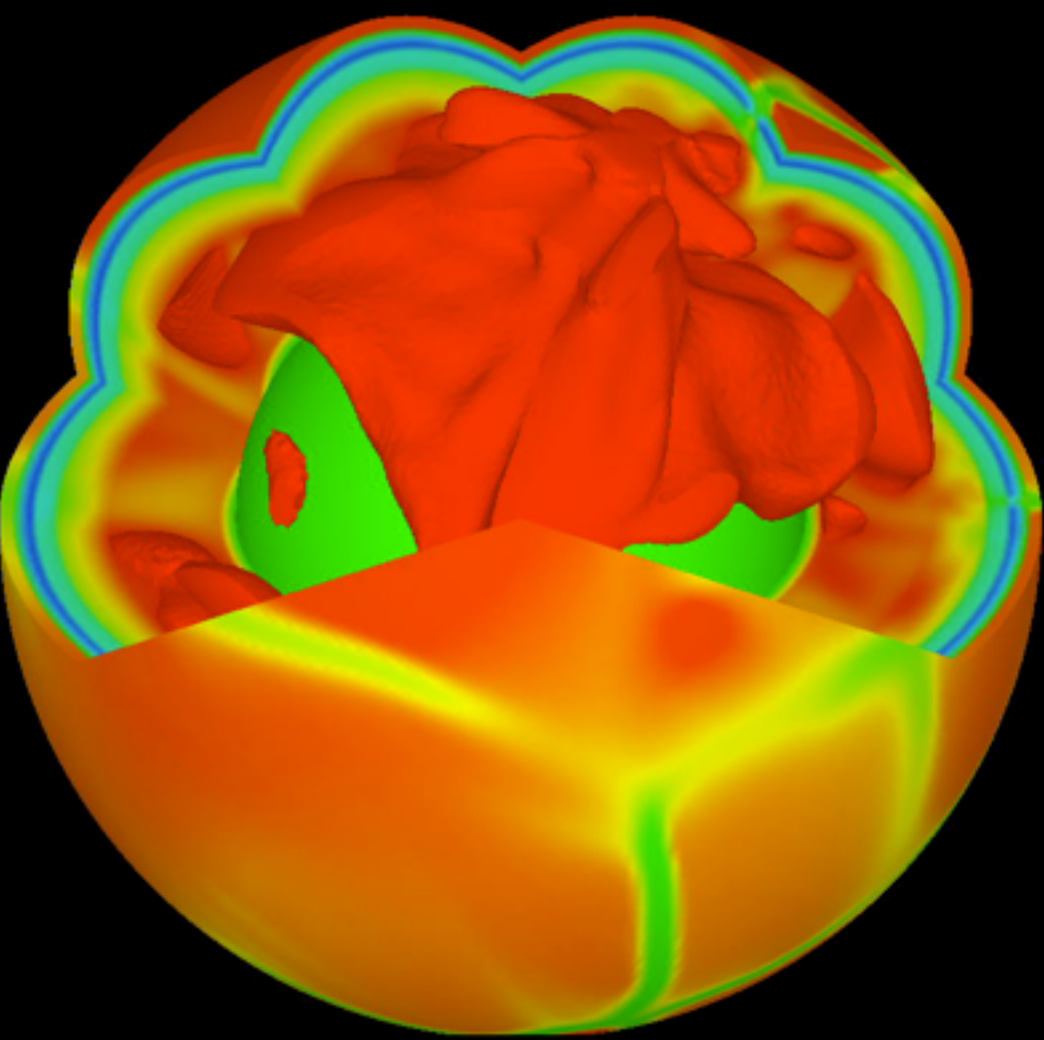

Mantle convection

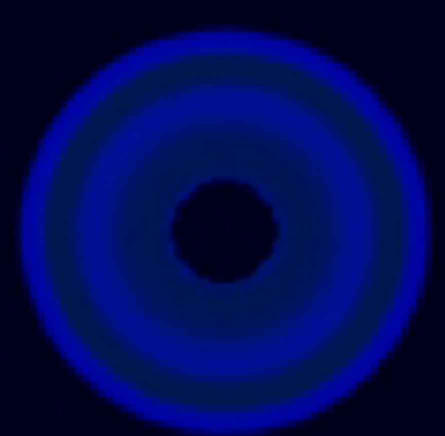

Neutrino-driven
convection in supernovae

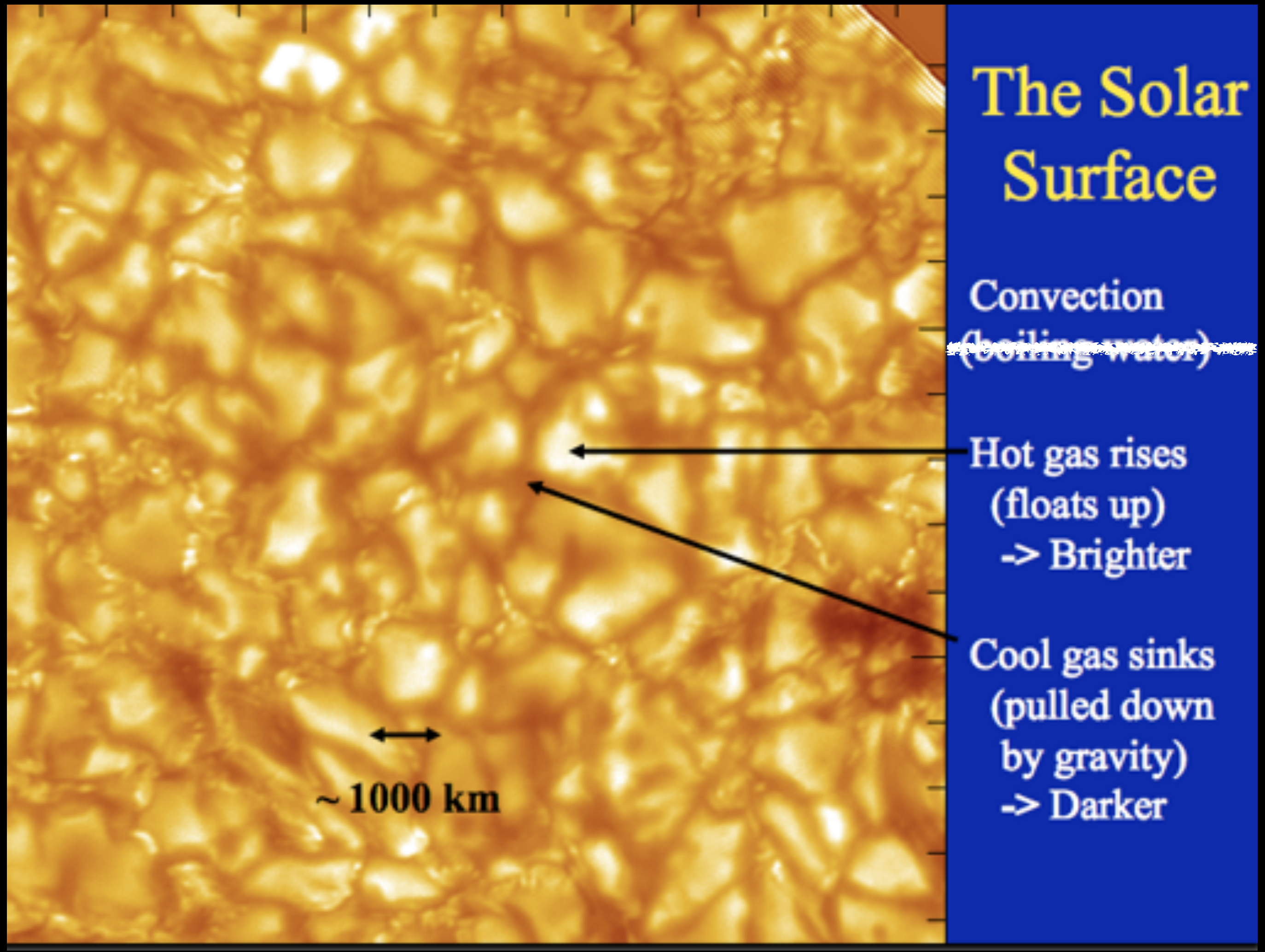

Stellar convection

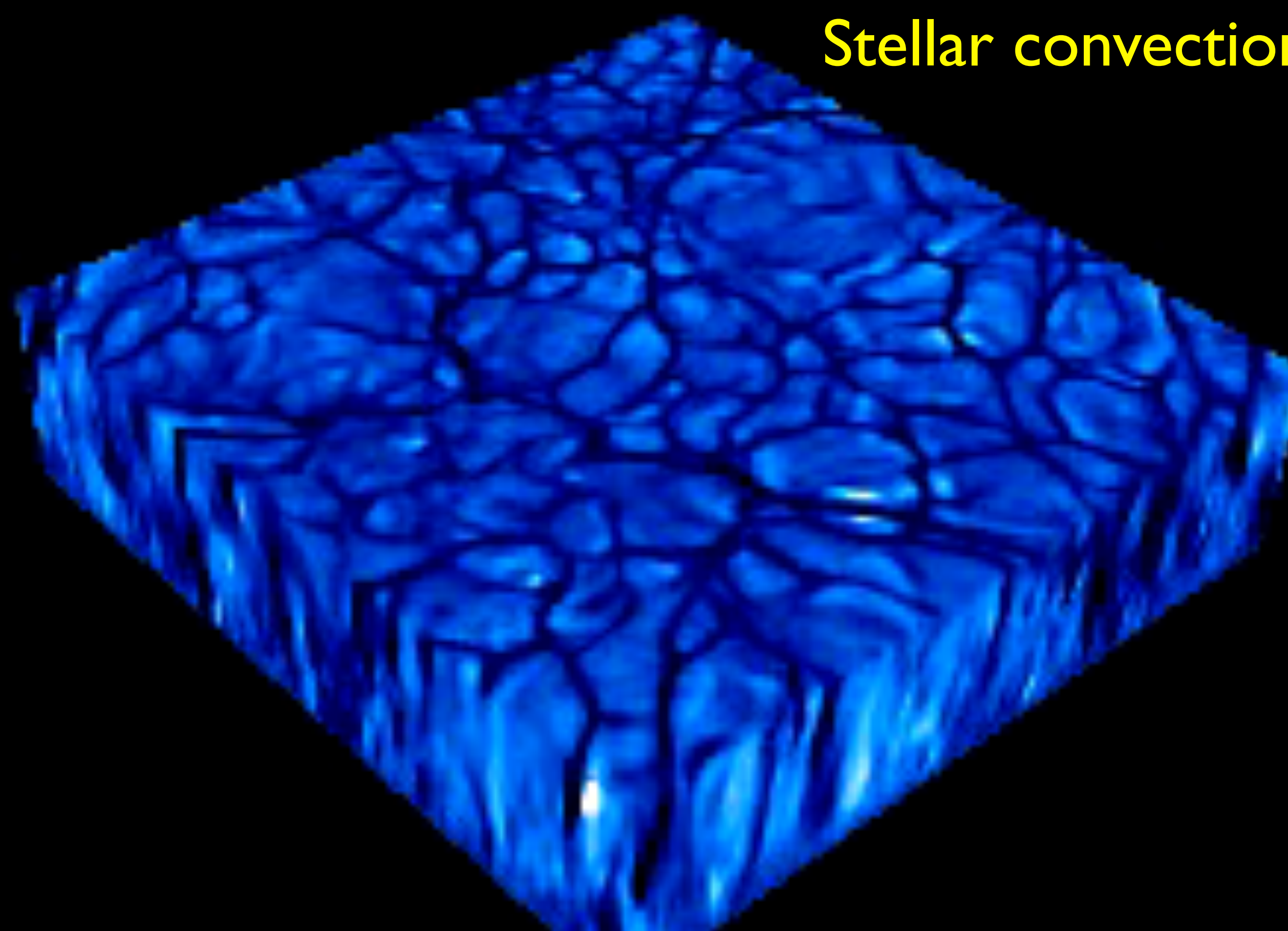

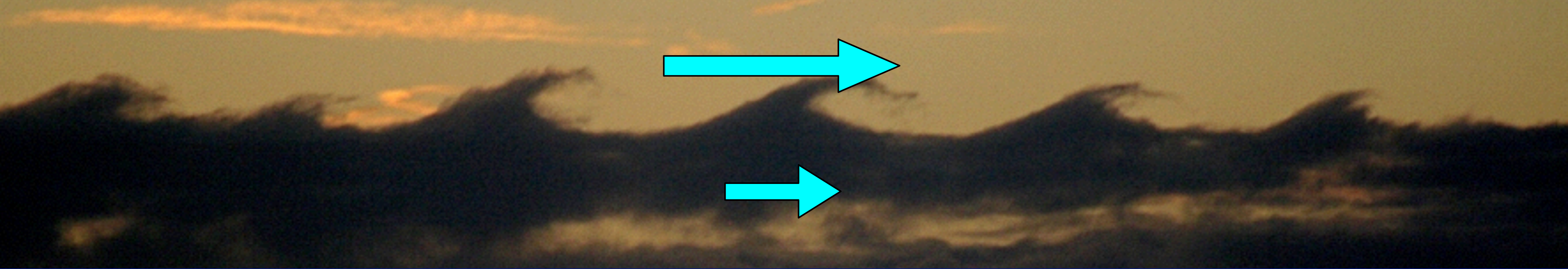

Necessary criterion for K-H instability in Cartesian shear flow:

$$\textit{Richardson } Ri \equiv \frac{\omega^2_{Brunt}}{(\partial v/\partial z)^2} < Ri_{\mathrm{crit}} = \frac{1}{4}$$

(see Shu for heuristic derivation)

$$= \frac{g\,\partial \ln \rho/\partial z}{(\partial v/\partial z)^2}$$

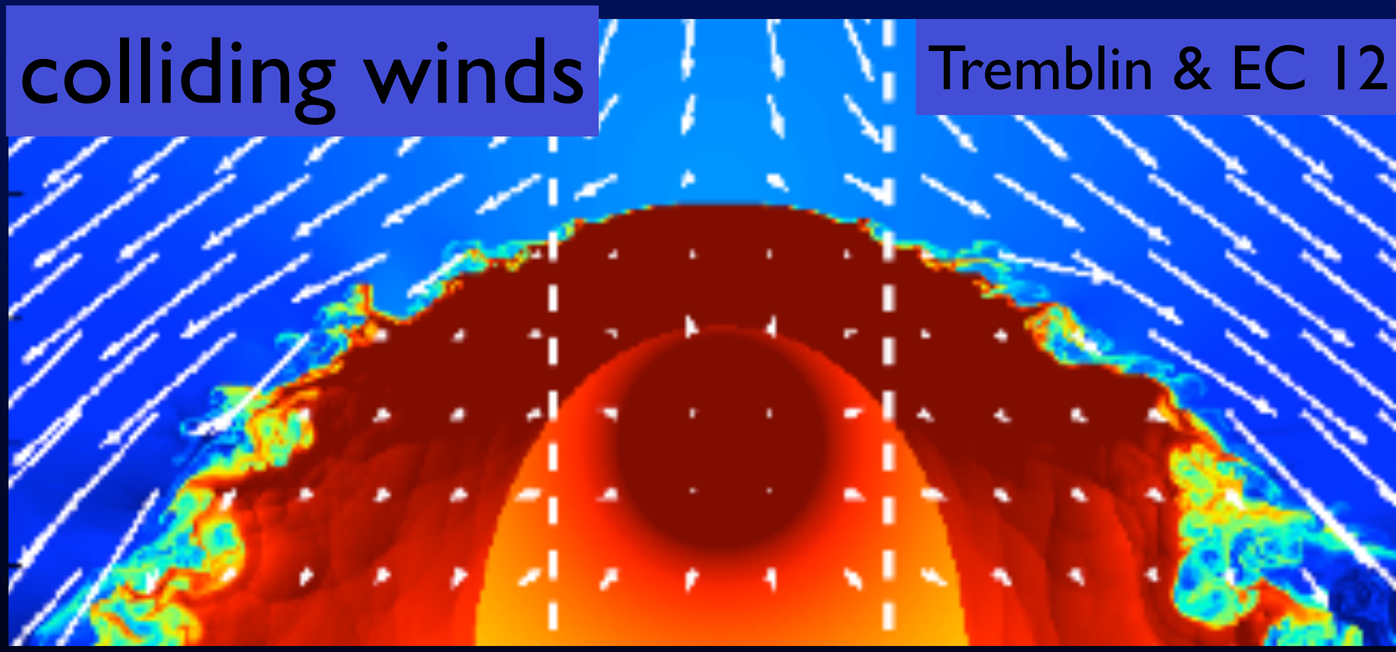

Kelvin-Helmholtz (KH) Instability:
Cartesian shear, if too strong, can overturn an otherwise stably stratified atmosphere (for formal linear analysis, including analysis of contact discontinuity in $\boldsymbol{\rho}$ and v, see Chandrasekhar 61)

Turbulent Cascade

Big whorls have little whorls,
which feed on their velocity.
Little whorls have lesser whorls,
and so on to viscosity.

Lewis Fry Richardson (cf. Jonathan Swift)

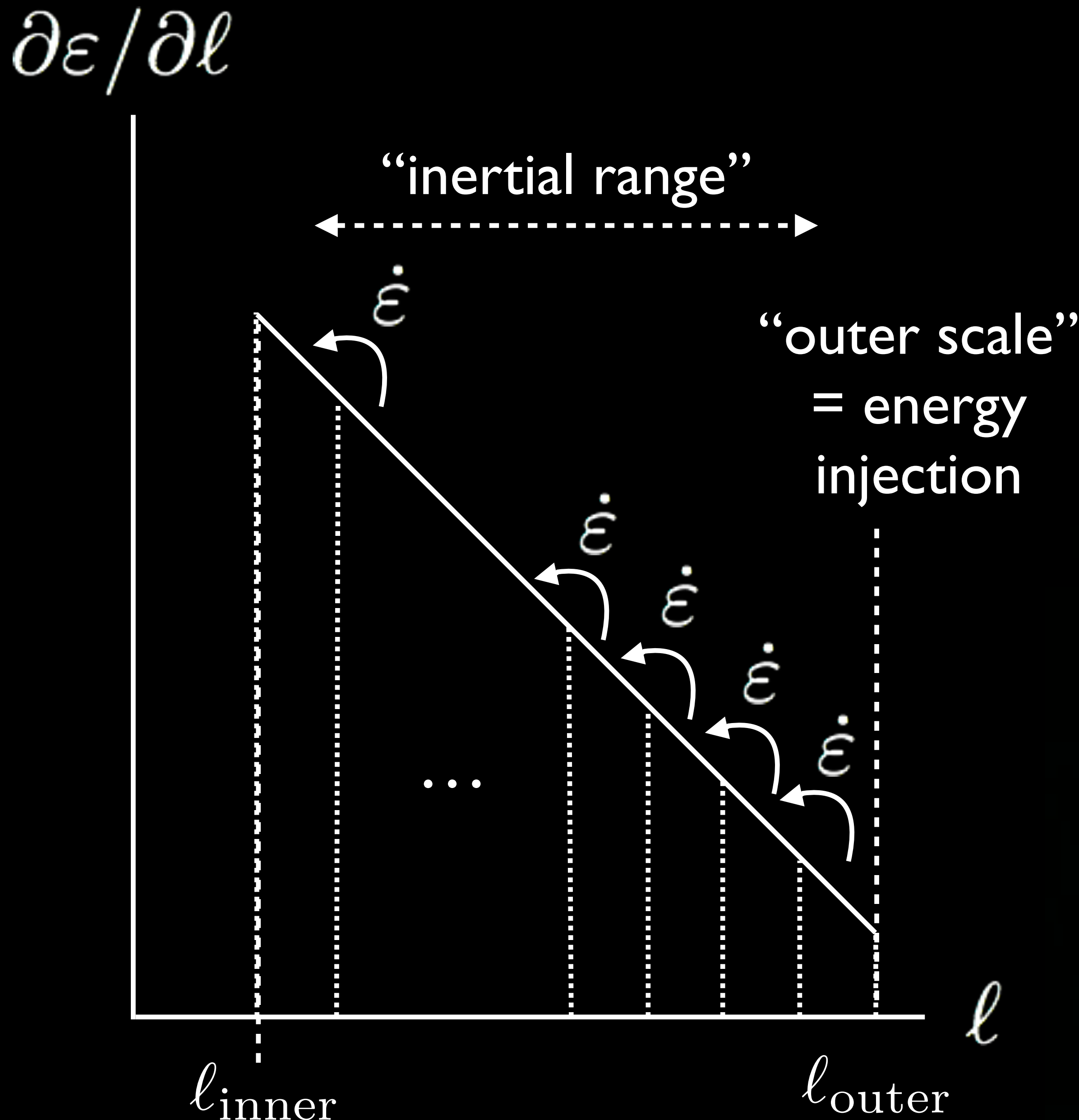

"inner scale"

= energy dissipation (energy goes into heat)